

## Original Article

# Molecular analysis of the early interaction between the grapevine flower and *Botrytis cinerea* reveals that prompt activation of specific host pathways leads to fungus quiescence

Zeraye Mehari Haile<sup>1,6</sup>, Stefania Pilati<sup>1</sup>, Paolo Sonego<sup>2</sup>, Giulia Malacarne<sup>1</sup>, Urska Vrhovsek<sup>3</sup>, Kristof Engelen<sup>2</sup>, Paul Tudzynski<sup>4</sup>, Michela Zottini<sup>5</sup>, Elena Baraldi<sup>6</sup> & Claudio Moser<sup>1</sup> 

<sup>1</sup>Genomics and Biology of Fruit Crops Department, Research and Innovation Centre, Fondazione Edmund Mach, Via E. Mach 1, San Michele all'Adige 38010, Trentino, Italy, <sup>2</sup>Computational Biology Department, Research and Innovation Centre, Fondazione Edmund Mach, Via E. Mach 1, San Michele all'Adige 38010, Trentino, Italy, <sup>3</sup>Food Quality and Nutrition Department, Research and Innovation Centre, Fondazione Edmund Mach, Via E. Mach 1, San Michele all'Adige 38010, Trentino, Italy, <sup>4</sup>Institute for Biology and Biotechnology of Plants, Westfälische Wilhelms-Universität Münster, Schlossplatz 8D-48143 Münster, Germany, <sup>5</sup>Department of Biology, University of Padua, Via U. Bassi 58/B, 35131 Padua, Italy and <sup>6</sup>Department of Agricultural Sciences, University of Bologna, Viale Fanin 46, 40127 Bologna, Italy

## ABSTRACT

**Grape quality and yield can be impaired by bunch rot, caused by the necrotrophic fungus *Botrytis cinerea*. Infection often occurs at flowering, and the pathogen stays quiescent until fruit maturity. Here, we report a molecular analysis of the early interaction between *B. cinerea* and *Vitis vinifera* flowers, using a controlled infection system, confocal microscopy and integrated transcriptomic and metabolic analysis of the host and the pathogen. Flowers from fruiting cuttings of the cultivar Pinot Noir were infected with green fluorescent protein (GFP)-labelled *B. cinerea* and studied at 24 and 96 hours post-inoculation (h.p.i.). We observed that penetration of the epidermis by *B. cinerea* coincided with increased expression of genes encoding cell-wall-degrading enzymes, phytotoxins and proteases. Grapevine responded with a rapid defence reaction involving 1193 genes associated with the accumulation of antimicrobial proteins, polyphenols, reactive oxygen species and cell wall reinforcement. At 96 h.p.i., the reaction appears largely diminished both in the host and in the pathogen. Our data indicate that the defence responses of the grapevine flower collectively are able to restrict invasive fungal growth into the underlying tissues, thereby forcing the fungus to enter quiescence until the conditions become more favourable to resume pathogenic development.**

*Key-words:* *Botrytis cinerea*; *Vitis vinifera*; defence response; quiescence.

## INTRODUCTION

Grapevine yield and quality face challenges worldwide from biotic stresses, mainly caused by fungi and oomycetes like *Botrytis cinerea*, *Plasmopara viticola* and *Erysiphe necator*. *B. cinerea*, a necrotroph responsible for pre-harvest and post-harvest diseases in many crops, causes bunch rot in grapevine. In vineyards, *B. cinerea* is part of the natural microflora where primary infections of berries are usually initiated by airborne conidia from overwintering sources (Nair *et al.* 1995; Elmer and Michailides 2004). Bunch rot frequently occurs on ripe berries close to harvest. Wet conditions together with damage to ripe berries, due to cuticle cracking from pressure within the berry/cluster and physical damage occurring during ripening, cause the expression of bunch rot, even though the primary infection could have occurred at earlier stages of berry development (McClellan and Hewitt 1973; Nair *et al.* 1995). Bunches inoculated at flowering were reported to have higher disease severity at maturity (Keller *et al.* 2003; Pezet *et al.* 2003b), implying that bunch rot disease observed during ripening may not only be due to *de novo* infection but also be due to latent infections that occurred at earlier stages of berry development. A similar infection strategy of the pathogen was also observed in strawberries and raspberries (Jarvis 1962; Williamson *et al.* 1987; Jersch *et al.* 1989). This delayed asymptomatic infection is known as quiescent infection.

Usually, *B. cinerea*, upon contact with the host, incites cell death by producing phytotoxins and cell-wall-degrading enzymes (CWDEs) and manipulates host metabolism to facilitate colonization (van Kan 2006; Choquer *et al.* 2007; Williamson *et al.* 2007). A deviation from this common necrotrophic lifestyle, where *B. cinerea* behaves as a facultative endophyte, has also been reported (Williamson *et al.* 1987; McNicol and Williamson 1989; Coertze and Holz 2002; van Kan *et al.* 2014; Shaw *et al.* 2016).

Corresponding author: C. Moser. e-mail: claudio.moser@fmach.it

In grapevine, *B. cinerea* infection often occurs at blooming and then remains quiescent until ripening (McClellan and Hewitt 1973; Nair *et al.* 1995; Keller *et al.* 2003; Pezet *et al.* 2003b). Berry developmental stages between bloom and véraison are mostly resistant to *B. cinerea* infection. Such development-related resistance could be linked to pre-formed and inducible antifungal compounds, as well as skin features of immature berries. Phenylpropanoid and flavonoid extracts of young berries, as well as resveratrol, can inhibit *B. cinerea* growth (Goetz *et al.* 1999; Schouten *et al.* 2002b; Pezet *et al.* 2003b). Furthermore, polyphenols in the berry skin cell wall and the thickness of epidermal cell layer complex were reported among the resistance factors (Mlikota-Gabler *et al.* 2003; Deytieux-Belleau *et al.* 2009). More recently, Agudelo-Romero *et al.* (2015) reported a large transcriptional activation of genes related to secondary metabolism and hormonal signalling [jasmonic acid (JA), ethylene (ET) and auxins] upon *B. cinerea* infection of immature berries of cultivar Trincadeira. Another study on grapes infected at véraison reported the accumulation of reactive oxygen species (ROS), the activation of the salicylic acid (SA)-dependent pathway and the induction of stilbene and lignin biosynthesis as defence mechanisms to arrest *B. cinerea* progression (Kelloniemi *et al.* 2015).

In disease management, quiescent infection has important implications for proper timing of prophylactic measures, to reduce stress factors that may trigger egression of the quiescent pathogen and to prolong quiescence to the point where the produce is not affected even after harvest (Jarvis 1994). Concerning grapevine, flowering is an important stage in the epidemiology of *B. cinerea* as infection at this stage is followed by quiescence. Therefore, understanding the interaction between *B. cinerea* and grapevine inflorescence is vital to implement proper management in order to limit consequent yield losses. Despite this, knowledge about the molecular mechanisms of the interplay between *B. cinerea* and grapevine inflorescences at bloom is lacking. Taking advantage of the availability of the genome sequences of *Vitis vinifera* (Jaillon *et al.* 2007; Velasco *et al.* 2007) and *B. cinerea* (Amselem *et al.* 2011; van Kan *et al.* 2016), we analysed the transcriptional alterations of both organisms during flower infection to understand the molecular mechanisms associated with the early stage of this interaction. Microscopic observation and metabolic profiles were combined with the transcriptomic analyses to further our understanding of the infection process at infection initiation and initial fungal quiescent stages.

## MATERIALS AND METHODS

### Plant material and *Botrytis cinerea* inoculation

Winter woody cuttings were collected from an experimental vineyard (*V. vinifera* cv. Pinot Noir) of the Fondazione Edmund Mach, Trentino-Alto Adige, Italy, and stored at 4 °C until use. Flowers were raised from the cuttings following the technique of Mullins and Rajaskekaren (1981). At EL17, according to Eichorn and Lorenz (1977), flowers were thinned to ensure that each flower could receive *B. cinerea* conidia. Cuttings were grown in a growth chamber at 24 °C, with a 16 h light cycle.

Transgenic *V. vinifera* plants (Microvine mutant) harbouring the H<sub>2</sub>O<sub>2</sub>-specific HyPer probe, targeted to the cytosol, were generated as described by Costa *et al.* (2010).

*Botrytis cinerea* (isolate B05.10) was cultured on potato dextrose agar (PDA, in Petri dishes) at 25 °C. After 10 d, conidia were harvested in distilled water and filtered with sterile pipette tip plugged with cotton wool. The concentration was determined using a haemocytometer. At full cap-fall stage (EL25/EL26), each flower was inoculated by positioning 1.5 µL of a  $2 \times 10^5$  mL<sup>-1</sup> conidia solution close to the receptacle area (Supporting Information Fig. S1). After inoculation, the whole cutting was bagged in a water-sprayed, clear plastic bag for 24 h to ensure high humidity, an essential factor for conidial germination.

For microscopic observation and post-inoculation evaluation (plating out test), a B05.10 transformant expressing a codon-optimized green fluorescent protein (GFP) (Leroch *et al.* 2011) under control of the constitutive oliC promoter from *Aspergillus nidulans*, named PoliC::GFP (Schumacher 2012), was used owing to its fluorescent signal and ability to grow on selective medium (PDA with 70 µg mL<sup>-1</sup> Hygromycin B). The construct is integrated at the bcniA locus, and the strain is homokaryotic.

### Microscopic observations and detection of quiescent *Botrytis cinerea*

Confocal laser scanning microscopy analyses were performed using a Leica SP5 imaging system (Leica Microsystems, Wetzlar, Germany) and a Zeiss LSM 700 (Carl Zeiss Microscopy, Jena, Germany). GFP and chlorophyll were excited at 488 nm, and the emission was collected at 515–560 and 650–750 nm, respectively. For HyPer detection, confocal microscopy analyses were performed according to Costa *et al.* (2010). Thin slices, which were manually cut from inoculated flowers, were subjected to microscopic observation.

For quiescent *B. cinerea* detection, the plating-out method on selective medium was used. Eight fruitlets from each of six biological replicates were sampled daily from 1 to 7 d and, at 14 d post-inoculation, were incubated on selective medium at room temperature for a week before or after washing or after surface sterilization. Washing was with sterile water, three rinses of 1 min each with gentle shaking, whereas surface sterilization was carried out with 70% ethanol (1 min) followed by 1% (vol/vol) NaClO (3 min) and three rinses in sterile water (Keller *et al.* 2003). Appearance of mycelial growth was scored as a confirmation of quiescent *B. cinerea* on the fruitlets. Fruitlets >4 mm in diameter (approximately) were cut into half before plating. Statistical significance was calculated by Tukey's honestly significant difference test on square-root-transformed data.

### Secondary metabolites and RNA extraction

Inflorescences from fruiting cuttings that were either mock or B05.10 conidia inoculated at the cap-off stage were collected at 12, 24, 48, 72 and 96 (h.p.i.), in three biological replicates,

immediately frozen in liquid nitrogen and kept at  $-80^{\circ}\text{C}$  until use. An inflorescence from a fruiting cutting was considered as a biological replicate. RNA was extracted using Plant Total RNA Kit (Sigma-Aldrich, St Louis, MO, USA) following the manufacturer's protocol. For polyphenol analysis, sample preparation and ultra-high-performance liquid chromatography–diode array detection–mass spectrometry (UHPLC-DAD-MS) analysis were conducted as described by Vrhovsek *et al.* (2012). The samples used for polyphenol and RNA extraction were independent.

For *B. cinerea* RNA extraction, B05.10 conidia were incubated in a flask with potato dextrose broth (PDB) for 12 h (Supporting Information Fig. S2) with 30 r.p.m. shaking in three biological replicates. Conidia obtained from a Petri dish were considered as a biological replicate.

### RNA sequencing, data processing and data analysis

Samples collected at 24 and 96 h.p.i. were used for RNA-Seq analysis. Approximately 20 million strand-specific, 100 bp long sequences were obtained for each sample using a next-generation sequencing platform HiSeq 1500 (Illumina, San Diego, CA, USA). The quality of the Illumina single-end reads was checked using FastQC (version 0.11.2) (<http://www.bioinformatics.babraham.ac.uk/projects/fastqc/>) and pre-processed for adapter with cutadapt (version 1.8.1) (Martin 2011). The resulting reads were aligned separately to the *B. cinerea* (strain B05.10) (<http://fungi.ensembl.org>) and the grapevine (12Xv1, <http://genomes.cribi.unipd.it/>) genomes using the Subread aligner (Liao *et al.* 2013). Raw read counts were extracted from the Subread alignments using the featureCount read summarization program (Liao *et al.* 2014). All raw RNA-Seq read data are deposited in the National Center for Biotechnology Information (NCBI) Short Read Archive (<http://www.ncbi.nlm.nih.gov/sra/>) under the BioProject accession code PRJNA336478 and Sequence Read Archive (SRA) accession code SRP080917.

Differential expression analysis was performed after the mean–variance relationship of the log counts was computed using the voom method (Law *et al.* 2014), which generates a precision weight for each observation to feed to the limma empirical Bayes analysis pipeline (Smyth 2004). Genes were considered differentially expressed (DE) if they fulfil a  $P$ -value  $< 0.05$  and an absolute fold change of  $\geq 1.5$ . Gene ontology enrichment was computed using customized annotation and annotated reference into the AgriGO analysis tool (<http://bioinfo.cau.edu.cn/agriGO/analysis.php>; Du *et al.* 2010). Enriched molecular networks ( $P < 0.05$ ) were identified using VESPUCCI (<http://vespucci.colombos.fmach.it>) (Moretto *et al.* 2016) based on VitisNet annotation (Grimplet *et al.* 2012). The MapMan tool (Thimm *et al.* 2004) was used to visualize DE genes in the context of biotic stress pathway using the GrapeGen 12Xv1 annotation version (Lijavetzky *et al.* 2012) as MapMan bins.

### Quantitative polymerase chain reaction

cDNA was synthesized from 3  $\mu\text{g}$  of the same RNA used for RNA-Seq analysis, treated with DNase I (Ambion, Austin, TX, USA), using the SuperScript™ VILO™ cDNA Synthesis Kit (Invitrogen, Carlsbad, CA, USA). Quantitative PCR (qPCR) was performed in a Viiia7 thermocycler (Applied Biosystems, Foster City, CA, USA) using 0.31  $\mu\text{L}$  of cDNA and 2.5  $\mu\text{M}$  of primers in a total volume of 12.5  $\mu\text{L}$  where half of the total volume was Fast SYBR Green Master Mix (Kapa Biosystems, Wilmington, MA, USA). Each amplification reaction was run in triplicate. For normalization, *VvACT* and *VvTUB*, and *BcRPL5* and *BcTUBA* genes were selected using GeNORM (Vandesompele *et al.* 2002) as reference for grapevine and *B. cinerea*, respectively. Amplification efficiencies of each primer pair were calculated with LinReg (Ruijter *et al.* 2009). The obtained amplification efficiency was used to calculate the relative quantity (RQ) and normalized RQ (NRQ) according to Hellemans *et al.* (2007). Statistical analyses of the qPCR results were made after  $\log_2(\text{NRQ})$  transformation (Rieu and Powers 2009). All primers and corresponding gene identifiers can be found in Supporting Information Data S1. Statistical significance was calculated by Tukey's honestly significant difference test or an unpaired heteroscedastic Student  $t$  test, considering each technical replicate as an individual sample.

### DNA extraction, standard curve and DNA quantification

DNA was isolated from grapevine flowers and *B. cinerea* (strain B05.10) mycelium, obtained from conidia incubated for 48 h as mentioned earlier, using the DNeasy Plant Mini Kit (Qiagen, Valencia, CA, USA) following the manufacturer's protocol. DNAs from mycelium and uninoculated grapevine flowers were used to generate calibration curves to estimate the amount of fungal DNA in inoculated samples. Samples were replicated three times.

Genomic DNA was used as a template for qPCR using primers *Bc3*, ribosomal intergenic spacer (IGS) and *VvRS I*, resveratrol synthase gene I, with similar amplification procedure described earlier. For the standard curve, qPCR reactions were carried out in triplicate from known fungal or plant DNA extracts, which were serially diluted five times. The standard curves were generated by plotting the log of DNA (pg) against the  $C_t$  value (Supporting Information Fig. S3). The  $C_t$  values obtained from inoculated samples were used to extrapolate the amount of genomic DNA from the standard curves. Genomic DNA of *B. cinerea* in a sample was normalized to the amount of grapevine genomic DNA in that sample.

## RESULTS

### *Botrytis cinerea* infection of grapevine flower

Artificial infection of grapevine flowers with a GFP-labelled B05.10 strain was conducted at full cap-off stage (EL25/

EL26) (Fig. 1a). The infection was monitored for 2 weeks post-inoculation (w.p.i.), and during this period, there were no visible symptoms of infection or fungal growth (Fig. 1b–e).

Although fungal conidia germination, formation of appressoria and penetration into the flower cuticle on the gynoecium were observed 24 h.p.i. (Fig. 1f and Supporting Information Fig. S4),

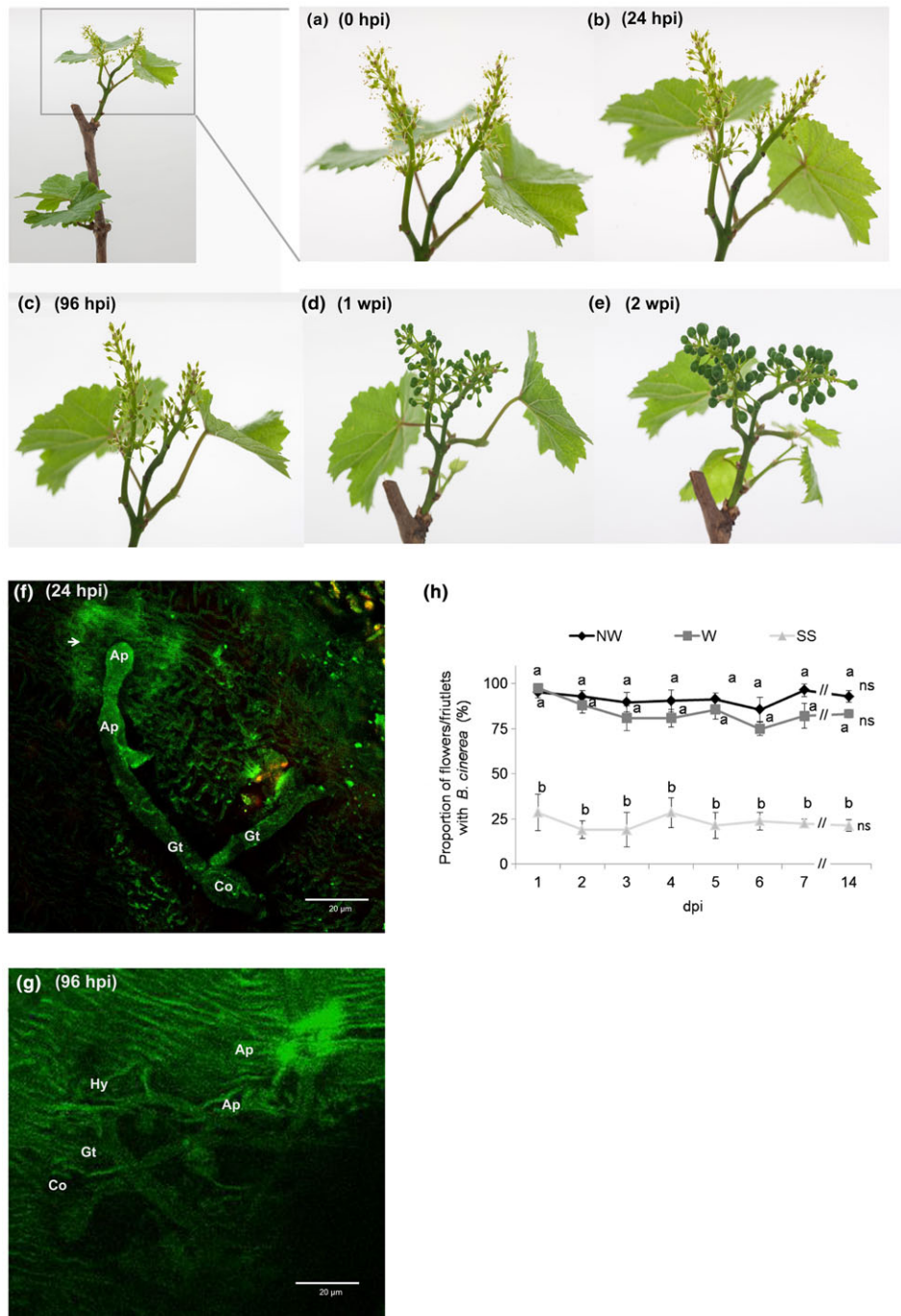


**Figure 1.** Grapevine flowers infected with *Botrytis cinerea*. Flowers inoculated with green fluorescent protein (GFP)-labelled B05.10 strain at the full cap-off stage (EL25/EL26), 0 hour post-inoculation (h.p.i.) (a) and asymptomatic inflorescence up to 2 weeks post-inoculation (b–e). (f, g) Confocal microscope images of GFP-labelled B05.10 infecting the cuticle of a grapevine flower 24 and 96 h.p.i. Ap, appressoria; Co, conidium; Gt, germ tube; Hy, hypha. Autofluorescence around penetration site (shown by arrow) indicates cell wall fortification. (h) Plating out of infected fruitlets on selective media (PDA with Hygromycin B,  $70 \mu\text{g mL}^{-1}$ ) to check the presence of quiescent *B. cinerea* on infected fruitlets before (NW) or after washing (W) or after surface sterilization (SS). d.p.i., days post-inoculation. Values at each day represent mean proportion of fruitlets (eight fruitlets from each of six biological replicates considered) showing GFP-labelled B05.10 growth on the selective media. Error bars indicate standard error. Mean proportions followed by a common letter within a d.p.i. are significantly not different among NW, W and SS, according to Tukey's honestly significant difference test ( $P \leq 0.05$ ), using one-way ANOVA. The mean proportions throughout the 2 weeks within NW, W or SS are not significantly different (n.s.).

no substantial growth progress was appreciated at 96 h.p.i. (Fig. 1g). The presence of viable fungus during 2 w.p.i. was confirmed by plating out experiments. Inoculated but healthy-looking fruitlets were incubated on selective media to allow the growth of the GFP-labelled *Botrytis* strain only. Germinated *B. cinerea* conidia were present on the skin of 90% of the inoculated fruitlets, whereas about 30% of the samples showed the presence of *B. cinerea* below the external cell layers of the fruitlet (Fig. 1h). A preliminary test confirmed that washing within 6 h.p.i. was able to remove ungerminated conidia from flowers and that surface sterilization abolished *B. cinerea* viability (Supporting Information Fig. S5).

To check if a similar load of *B. cinerea* was present at different post-inoculation times, the amount of fungal and grapevine DNA was estimated by quantifying *Bc3* and *VvRS I* genes, respectively (Supporting Information Fig. S3a,b). As shown in Fig. 2a, the relative amount of fungal DNA compared to plant DNA ranged from 4 to 6%, with a slight increase within 2 d.p.i., indicating initial pathogen growth, followed by a slight decrease possibly associated to a quiescent state. Furthermore, the expression profile of *B. cinerea* actin, an indicator of active growth, confirmed that the growth of the fungus was relatively high up to 2 d.p.i. and then decreased slightly but significantly, supporting pathogen quiescence (Fig. 2b).

Inoculated inflorescences were inspected until ripening. At full colouring (approximately 10 w.p.i.), bunches were either bagged with plastic bags, to create favourable humidity for *B. cinerea*, or left as such. Two weeks after bagging, egression of *B. cinerea* was observed on about 40% of the inoculated berries (Supporting Information Fig. S6a). Cross-checking of the fungal strain, using a fluorescence microscope, confirmed that it was the GFP-labelled B05.10 strain inoculated at the cap-off stage (Supporting Information Fig. S6b). On the other hand, no egression was observed from unbagged bunches. To see if bagging can trigger egression before maturity, bunches at the peppercorn stage, which were infected at the cap-off stage, were bagged for 2 weeks, but no egression was observed (Supporting Information Fig. S7).

### Transcriptome analysis of infected grapevine flowers

Three biological replicates of mock-inoculated or B05.10-inoculated flowers were harvested at 24 and 96 h.p.i. for dual (plant and fungus) RNA-Seq analysis. These time points were chosen to understand the process of infection initiation (24 h.p.i.) and progress (96 h.p.i.), if any. The fraction of reads from *Botrytis*-inoculated and mock-inoculated flowers mapped to the grapevine reference genome was between 65 and 82%, whereas only up to 4.6% could be mapped to the *B. cinerea* genome (Supporting Information Data S2). In the case of *B. cinerea*, cultured in PDB, used as the control sample, about 90% of reads were mapped to the fungal genome, suggesting that the scarce number of fungus reads derived from the infected flowers is likely caused by the low number of conidia

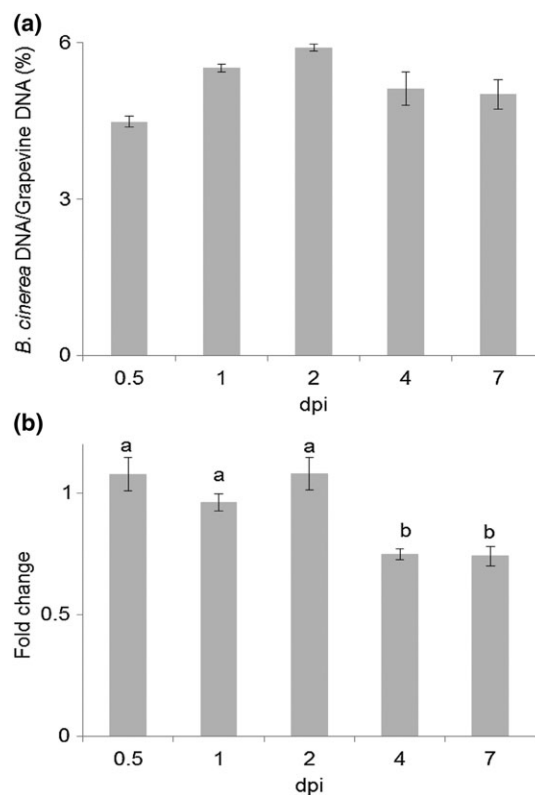


**Figure 2.** Relative quantification of genomic DNA and expression profile of actin gene from *Botrytis cinerea* at different days post inoculation (d.p.i.). (a) Amount of *B. cinerea* gDNA relative to grapevine gDNA, measured by amplification of the *B. cinerea* gene *Bc3* [ribosomal intergenic spacer (IGS)] and the grapevine gene *VvRS I* (resveratrol synthase gene I) on gDNA from *Botrytis*-inoculated flowers. The Kruskal–Wallis one-way ANOVA test revealed that the amount of *B. cinerea* gDNA at different d.p.i. is not significantly different,  $P = 0.123$ . Error bar represents standard error of the mean of three biological replicates. (b) Relative expression of a *B. cinerea* actin gene, *BcACTA*, to monitor the growth of the pathogen *in planta*. Bars represent fold change of inoculated samples relative to potato dextrose broth (PDB)-cultured *B. cinerea* (control). Normalization based on the expression levels of ribosomal protein L5, *BcRPL5*, and  $\alpha$ -tubulin, *BcTUBA*, was carried out before calculating fold changes. Expression values followed by the same letter are significantly not different between samples, according to Tukey's honestly significant difference test ( $P \leq 0.05$ ), using one-way ANOVA on  $\log_2(\text{NRQ})$ .

used for the infection (around 300) and of the limited fungal growth after inoculation.

As for grapevine, the biological variability within replicates and among experimental conditions was analysed by principal component analysis (PCA). As shown in Fig. 3a, the first principal component separates the two time points (24 and 96 h.p.i.) and also the 24 hours' *Botrytis*-treated versus untreated samples. In contrast, all samples collected at 96 h.p.i. seem very similar at a whole transcriptome level, as indicated by the large overlap in the PCA.

Differential expression of grapevine genes was calculated between *Botrytis*-inoculated versus mock-inoculated flowers (Supporting Information Data S3) within each time point. At 24 h.p.i., 1193 genes were DE (up-regulated or down-regulated), whereas at 96 h.p.i. only 265 genes were DE

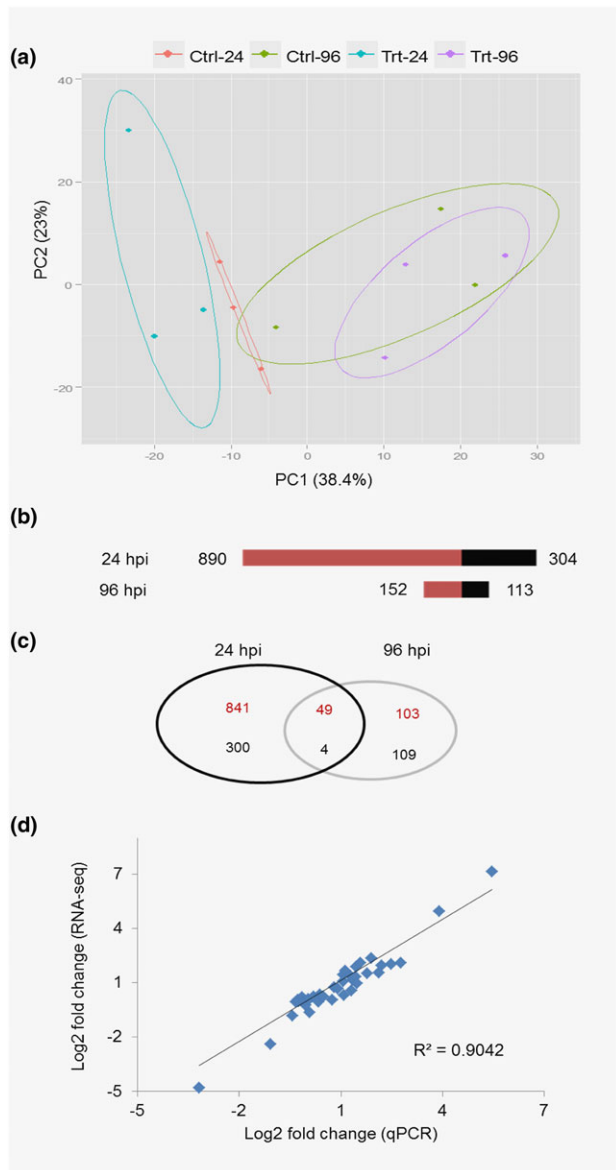


**Figure 3.** Analysis of the RNA-Seq data and of the differentially expressed (DE) genes. (a) Principal component analysis (PCA) displaying the biological variations among samples. Ctrl, mock inoculated; Trt, *Botrytis cinerea* inoculated; Bc, *B. cinerea*; 1–3 indicate the three biological replicates; 24 and 96 indicate hours post inoculation (h.p.i.). Raw count data were used after precision weight was calculated by the voom method (Law *et al.* 2014). (b) Number of DE genes ( $P < 0.05$ , fold change  $> 1.5$ ) upon *B. cinerea* infection at 24 and 96 h.p.i.; up-regulated genes (red) and down-regulated genes (black). (c) Venn diagram showing the number of DE genes unique or common to 24 and 96 h.p.i. (d) Validation of RNA-Seq data by qPCR assay: correlation of fold change values for 20 *Vitis* genes obtained by RNA-Seq and quantitative PCR (qPCR).

(Fig. 3b, Supporting Information Fig. S8 and Supporting Information Data S4). The overlap between the two sets was limited to 49 up-regulated and four down-regulated genes (Fig. 3c). Interestingly, at 24 h.p.i., the plant seems to respond to the presence of the pathogen with a prevalent induction of genes, which appeared to be no longer modulated at 96 h.p.i.

Gene expression values from RNA-Seq analysis were validated using qPCR assay. The expression measurement of 20 grapevine genes (Supporting Information Data S5) by qPCR was in very good agreement ( $R^2 > 0.90$ ) with the results obtained by RNA-Seq (Fig. 3d).

### Defence-related responses are largely induced in the flower upon *B. cinerea* infection

Differentially expressed genes were annotated according to the Gene Ontology (GO) (<http://genomes.cribi.unipd.it/grape/>) and VitisNet (<https://www.sdstate.edu/ps/research/vitis/pathways.cfm>) databases. GO functional class enrichment and VitisNet analysis provided consistent and complementary results (Table 1 and Supporting Information Data S6). A clear regulation of those classes typically modulated during biotic stress responses was found, as depicted in the MapMan pathway (Fig. 4) and in the enriched set of *Botrytis*-infected flowers (Supporting Information Data S7). In the following text, these classes are presented in detail.

One of the earliest cellular responses following plant–pathogen interaction is the production of ROS. Upon *B. cinerea* infection, genes encoding enzymes involved in oxidative stress such as glutathione *S*-transferase (GST), ascorbate oxidase, 2OG-Fe(II) oxygenase and cytochrome P450 monooxygenases were strongly up-regulated (Table 2 and Supporting Information Data S8). ROS accumulation at 24 h.p.i. was proven by a localized green fluorescence emitted at the site of penetration in flowers obtained from a cytoplasmic HyPer (cHyPer) transgenic line (Fig. 5).

Several genes encoding membrane-localized receptor-like kinases (RLKs), such as *CLV1*, *WAK1* and *BAK1*, which have been characterized in connection with immune responses to necrotrophic pathogens (Kemmerling *et al.* 2007; Brutus *et al.* 2010), were also up-regulated at 24 h.p.i. (Supporting Information Data S8). Genes associated with phytohormones, known to be involved in pathogen response signalling, were also DE (Fig. 4 and Table 1). According to the number of DE genes related to ET biosynthesis or signalling, this hormone seems to be important in the interaction between grapevine flower and *B. cinerea*. Two *ACC synthase* and one *ACC oxidase* genes in addition to seven ET-responsive transcription factors (TFs) were DE (Supporting Information Data S8). In addition, genes encoding an SA marker *PRI* and the plant defence regulator involving SA signalling *EDSI* (Wiermer *et al.* 2005) were up-regulated in the infected sample at 24 h.p.i. (Table 2). Jasmonate ZIM-domain gene, a marker for JA, was also up-regulated. Other genes involved in the synthesis of and signalling by phytohormones (apart from ET, JA and SA pathways) showed changes in transcript levels following inoculation with *B. cinerea*, suggesting a complex hormonal interplay. For example, five genes encoding nitrilase and nitrile hydratases, involved in indole-3-acetic acid synthesis, were differentially regulated, as well as receptor genes for gibberellic acid (GA) and abscisic acid (ABA) (Supporting Information Data S2). The global hormonal alterations

**Table 1.** Enriched grapevine molecular networks according to VitisNet annotation

VVID	Network name	Description	Number in input list	Number in reference list	P-value
<i>Up-regulated genes (24 h.p.i.)</i>					
10530	Amino sugar metabolism	Carbohydrate metabolism	9	76	1.15E-03
10910	Nitrogen metabolism	Energy metabolism	8	83	2.04E-03
10350	Tyrosine metabolism	Amino acid metabolism	10	130	3.23E-03
10460	Cyanoamino acid metabolism	Other amino acid metabolism	4	31	9.99E-03
10480	Glutathione metabolism	Other amino acid metabolism	16	127	4.14E-07
10770	Pantothenate and coenzyme A (CoA) biosynthesis	Cofactors and vitamin metabolism	5	39	4.16E-03
10940	Phenylpropanoid biosynthesis	Biosynthesis of secondary metabolites	40	187	2.00E-12
11000	Single reactions	Other	11	154	3.65E-03
34020	Calcium signalling pathway	Signal transduction	9	128	9.05E-03
30008	Ethylene signalling	Hormone signalling	15	232	2.00E-03
34626	Plant-pathogen interaction	Plant-specific signalling	25	311	1.75E-06
60003	AP2/EREBP	Transcription factor	10	131	3.41E-03
60066	WRKY	Transcription factor	19	62	1.93E-11
60069	ZIM	Transcription factor	4	13	3.36E-04
<i>Down-regulated genes (24 h.p.i.)</i>					
10500	Starch and sucrose metabolism	Carbohydrate metabolism	12	324	2.71E-04
44110	Cell cycle	Cell growth and death	21	316	3.85E-11
44810	Regulation of actin cytoskeleton	Cell motility	27	340	5.85E-16
60076	Other GTF		2	6	1.79E-03
<i>Up-regulated genes (96 h.p.i.)</i>					
10640	Propanoate metabolism	Carbohydrate metabolism	4	63	6.66E-04
50121	Porters cat 1 to 6	Transporter catalogue	6	160	5.20E-04
<i>Down-regulated genes (96 h.p.i.)</i>					
40006	Cell wall	Cell growth and death	12	445	1.31E-07

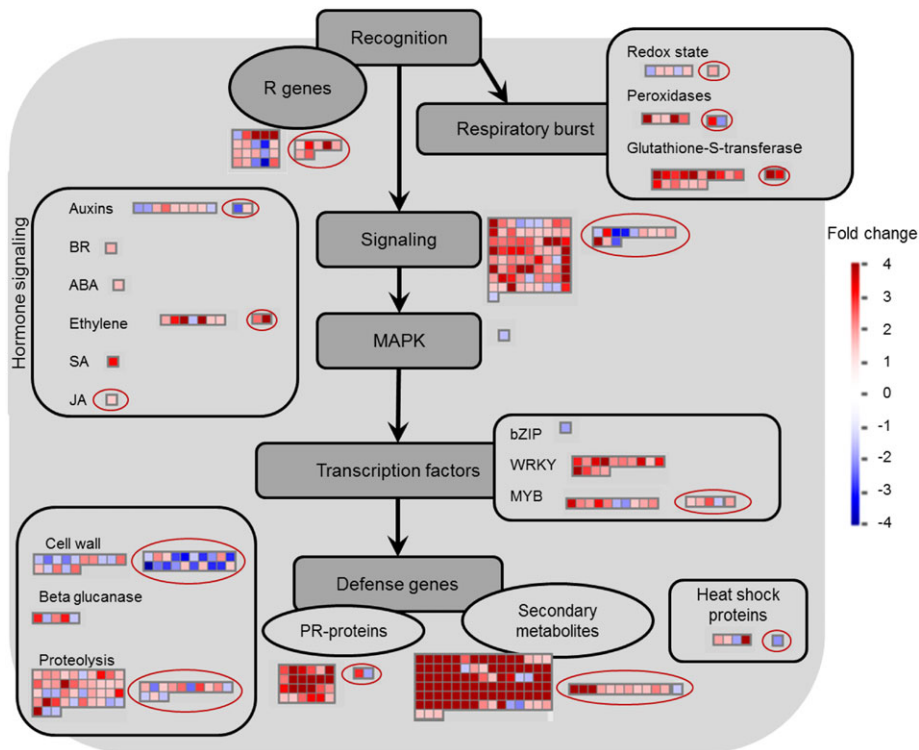


**Figure 4.** MapMan overview of biotic stress in inoculated flower at 24 and 96 hours post-inoculation (h.p.i.) (red circle). Up-regulated and down-regulated genes are shown in red and blue, respectively. The scale bar displays fold change values. ABA, abscisic acid; BR, brassinosteroid; JA, jasmonic acid; MAPK, mitogen-activated protein kinase; SA, salicylic acid. The list of MapMan enriched pathways within differentially expressed (DE) genes is provided in Supporting Information Data S7.

**Table 2.** Selected differentially expressed grapevine genes from *B. cinerea* inoculation at 24 and 96 h.p.i.

ID	Fold change (log2)		Functional annotation
	24 h.p.i.	96 h.p.i.	
<i>Recognition and signalling</i>			
VIT_15s0046g02220	2.67		ACC synthase
VIT_07s0031g01070	2.21		Ascorbate oxidase
VIT_14s0030g02150	2.04	2.33	Calmodulin
VIT_11s0016g03080	1.42		Clavata1 receptor kinase (CLV1)
VIT_12s0035g00610	6.01		CYP82M1v3
VIT_18s0001g00030	1.01	2.79	CYP87A2
VIT_17s0000g07400	1.01		Disease resistance protein (EDS1)
VIT_17s0000g07420	1.38		Enhanced disease susceptibility 1 (EDS1)
VIT_02s0234g00130	1.60		Ethylene responsive element binding factor 1
VIT_15s0048g01350	2.22		Gibberellin receptor GID1L3
VIT_08s0040g00920	2.94	1.71	Glutathione <i>S</i> -transferase 25 GSTU7
VIT_11s0016g00710	0.83		Jasmonate ZIM-domain protein 1
VIT_01s0011g03650	2.21		Map kinase substrate 1 MKS1
VIT_00s0250g00090	4.42	2.72	Oxidoreductase, 2OG-Fe(II) oxygenase
VIT_03s0063g02440		-1.71	Proline extensin-like receptor kinase 1 (PERK1)
VIT_13s0064g01790	-1.62		R protein MLA10
VIT_00s0748g00020	4.14		Receptor kinase RK20-1
VIT_17s0000g04400	1.38		Wall-associated kinase 1 (WAK1)
<i>Transcription factors</i>			
VIT_07s0005g03220	3.53		ERF098
VIT_11s0016g02070	3.09	1.43	Basic helix-loop-helix (bHLH) family
VIT_07s0005g03340	1.87		Myb domain protein 14
VIT_19s0027g00860	3.64		NAC domain-containing protein 42
VIT_08s0058g00690	1.65		WRKY DNA-binding protein 33
VIT_14s0068g01770	3.29		WRKY DNA-binding protein 75
<i>Cell wall</i>			
VIT_14s0128g00970	2.75	1.40	Germin-like protein 3
VIT_05s0077g01280	-1.72	-2.40	Glycosyl hydrolase family 3 beta xylosidase (BXL1)
VIT_06s0009g02560	3.21		Pectinesterase family
VIT_08s0007g08330	-4.80		Polygalacturonase PG1
VIT_09s0054g01080	3.10		Polygalacturonase QRT3
VIT_06s0004g01990	4.87	3.15	Proline-rich extensin-like family protein
VIT_03s0017g01990	1.79		UDP-glucose glucosyltransferase
<i>Response to stress and secondary metabolism</i>			
VIT_18s0001g04280	5.07		(-)-Germacrene D-synthase
VIT_11s0052g01110	1.96		4-Coumarate-CoA ligase 1
VIT_04s0008g07250	2.04		Aspartyl protease
VIT_05s0077g01540	5.43		Bet v I allergen
VIT_16s0098g00850	0.68		Caffeic acid <i>O</i> -methyltransferase
VIT_16s0100g00860	4.99		Chalcone synthase
VIT_11s0149g00280	2.13		Chitinase A
VIT_03s0180g00250	4.41		Cinnamyl alcohol dehydrogenase
VIT_16s0039g02350	1.07		Dihydroflavonol 4-reductase
VIT_18s0122g01150	6.57	2.61	Diphenol oxidase
VIT_06s0004g01020	5.62	2.10	Dirigent protein
VIT_07s0031g01380	2.04	0.96	Ferulate 5-hydroxylase
VIT_05s0020g05000	1.70		Inhibitor of trypsin and hageman factor (CMTI-V)
VIT_18s0001g00850	6.48	2.84	Laccase
VIT_16s0098g00460	3.29		Lipase class 3
VIT_14s0083g00850		-1.67	Lipase GDSL 7
VIT_13s0067g00050	3.32		Myrcene synthase
VIT_15s0048g02430	1.65		Naringenin-2-oxoglutarate 3-dioxygenase
VIT_05s0077g01530	4.94	1.56	Pathogenesis protein 10
VIT_05s0077g01550	4.62		Pathogenesis protein 10.3
VIT_03s0088g00750	1.45		Pathogenesis-related protein 1 precursor
VIT_01s0010g02020	7.12	2.09	Peroxidase
VIT_16s0039g01280	5.40		Phenylalanine ammonia lyase
VIT_00s2849g00010	5.83		Phenylalanine ammonia lyase
VIT_02s0025g02920	1.67		Quercetin 3- <i>O</i> -methyltransferase 1
VIT_08s0058g00790	1.51		Secoisolariciresinol dehydrogenase
VIT_16s0100g01010	4.64		Stilbene synthase (VvSTS29)
VIT_16s0100g01130	4.34		Stilbene synthase (VvSTS41)
VIT_16s0100g01160	4.39		Stilbene synthase (VvSTS45)
VIT_16s0100g00990	4.60		Stilbene synthase 2 (VvSTS27)
VIT_16s0100g00950	4.63		Stilbene synthase 3 (VvSTS25)
VIT_02s0025g04230	2.21		Thaumatococin
VIT_11s0065g00350	3.54		<i>Trans</i> -cinnamate 4-monooxygenase



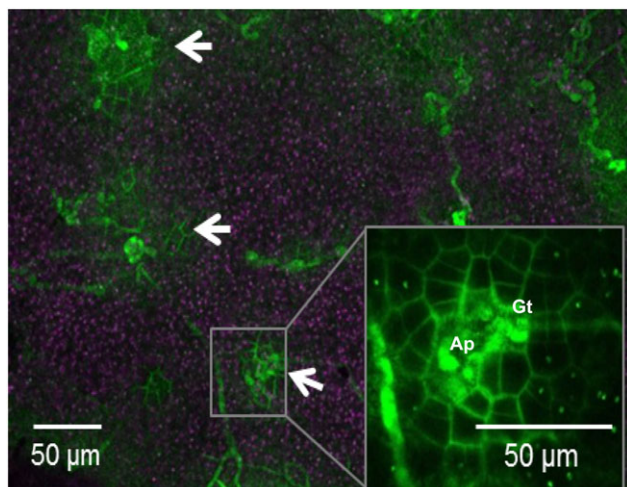


**Figure 5.** Confocal image of cytoplasmic HyPer grapevine transgenic flowers infected with *Botrytis cinerea*. A higher intensity of HyPer fluorescence is evident 24 hours post-inoculation (h.p.i.) at the penetration site of *B. cinerea*, compared with the rest of the plant tissue, indicating a localized and specific H<sub>2</sub>O<sub>2</sub> accumulation (shown by arrows). The inset at higher magnification clearly shows that the bright signal comes from the cytosol of proximal cells to the site of infection.

related to infection were evaluated by HORMONOMETER software (Volodarsky *et al.* 2009), which also suggested the involvement of several hormones (Supporting Information Fig. S9).

Following the *Botrytis*-induced signalling cascades, about 100 TFs were DE in infected flowers. Most prominent were genes encoding WRKY, MYB, ET-responsive element-binding proteins and NAC TFs (Supporting Information Data S8). Among the transcriptional regulators previously associated to the defence reaction were *WRKY33*, a transcriptional regulator involved in defence against *B. cinerea* and *P. viticola* (Birkenbihl *et al.* 2012; Merz *et al.* 2015), and *Myb14*, which in grapevine regulates stilbene biosynthesis (Höll *et al.* 2013). This fast and strong induction of specific TFs leads to the activation of specific pathways, clearly related to plant defence. A number of genes encoding different classes of PR proteins, such as chitinase, Bet v I allergen and  $\beta$ -1,3-glucanase were up-regulated, up to 40-fold. In this work, the transcription levels of *VvPR10.1* and *VvPR10.3*, and their regulator *WRKY33*, as indicated by previous studies for *VvPR10.1* (Dadakova *et al.* 2015; Merz *et al.* 2015), were analysed in more detail. The transcription profiles measured by qPCR at five time points within the first 96 h.p.i. revealed that the transcript level of *VvWRKY33* was higher at 12 and 24 h.p.i. (as compared to mock-treated samples) and dropped to the control level at later time points, 48 h.p.i. and beyond, while the PR proteins were always higher than control, except *VvPR10.1* at 48 h.p.i. (Fig. 6). Proteases including those involved in defence such as subtilisin-like protease, aspartic protease and serine protease inhibitor were also more expressed in *Botrytis*-inoculated than in mock-treated flowers (Supporting Information Data S8).

## Secondary metabolism, mainly related to polyphenols, is up-regulated in infected flowers

The RNA-Seq results underlined a reprogramming in secondary metabolism, especially at 24 h.p.i. (Fig. 4 and Supporting Information Data S8). Several genes related to terpenoid, benzoic acids, monolignol precursors, stilbenoid and flavonoid biosynthesis were strongly up-regulated at 24 h.p.i. From the enrichment analysis, secondary metabolic process, protein modification process and phenylpropanoid biosynthesis were among the enriched functional categories (Table 1 and Supporting Information Data S6). To confirm these RNA-Seq observations, targeted secondary metabolites, mainly polyphenols, were quantified by UHPLC-DAD-MS at five time points between 12 and 96 h.p.i. The analysis revealed that different classes of polyphenols were detected at higher concentrations in *Botrytis*-infected flowers as compared to mock-treated flowers (Supporting Information Data S9), suggesting a defence-oriented metabolome reprogramming. Figure 7 shows a heat map of the concentrations of metabolites in correlation with gene expression profiles, taken from the RNA-Seq result. In the phenylpropanoid pathway, 10 genes encoding *PAL* were up-regulated, between 13-fold and 55-fold at 24 h.p.i. (Supporting Information Data S8). Furthermore, genes encoding key enzymes in the pathway cinnamate-4-hydroxylase (*C4H*) and 4-coumarate-coenzyme A (*CoA*) ligase (*4CL*) had a fold change of about 12 and 4 times, respectively (Table 2). The concentrations of benzoic acids (*p*-hydroxybenzoic acid, vanillic acid and gallic acid) and monolignol precursors (ferulic acid, caftaric acid, fertaric acid and *trans*-coutaric acid) were generally higher in infected flowers (Fig. 7a).

Regarding stilbenoid biosynthesis, a number of stilbene synthase (*STS*) genes were highly up-regulated at 24 h.p.i. (Supporting Information Data S8). Of the 46 grapevine genes encoding for *STS*, more than 80% of them were expressed in the infected flowers with a relative induction between 15-fold and 90-fold. Two genes encoding *VvMYB14*, a TF regulating stilbene biosynthesis (Höll *et al.* 2013), were also up-regulated at 24 h.p.i. (Table 2), suggesting that this regulatory circuit is activated at 24 h.p.i. The expression profiles of *VvMYB14* and two *STS* genes, *VvSTS29* and *VvSTS41*, were further monitored using qPCR (Fig. 7b). Because of sequence similarity among *STS* genes (Vannozzi *et al.* 2012), the primers used for *VvSTS29* also detect the isoforms *VvSTS25* and *VvSTS27*, while the primers used for *VvSTS41* detect the isoform *VvSTS45* too (Höll *et al.* 2013). These results showed a strong coinduction between the *STS* genes and *VvMYB14* in grapevine flowers/fruitlets in response to *B. cinerea* infection. The expression patterns observed in the qPCR assay also fitted with the quantification of stilbenoids. The phytoalexin resveratrol and its monomeric derivatives piceatannol and *trans*-piceid were detected at higher concentrations in the infected flowers/fruitlets than control (Fig. 7a). The other monomers astringin and isorhapontin, both tetrahydroxystilbenes with antifungal activity (Hammerbacher *et al.* 2011), were also induced. All of the quantified oligomeric resveratrols (dimers: *trans*- $\epsilon$ -viniferin,

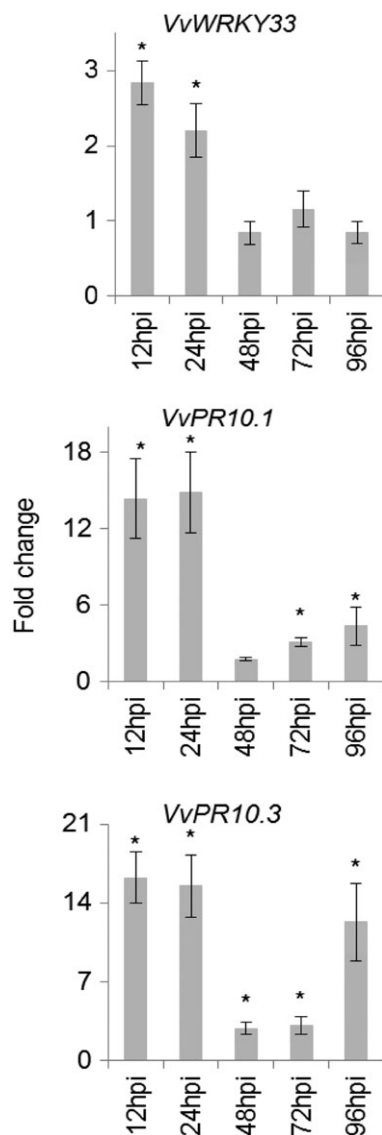


**Figure 6.** Expression profiles of *VvWRKY33*, *VvPR10.1* and *VvPR10.3* following *Botrytis cinerea* inoculation. Gene expression levels were determined by quantitative PCR (qPCR). Bars represent fold change of inoculated samples relative to mock-inoculated samples at each post-inoculation time. Normalization based on the expression levels of actin, *VvACT*, and tubulin, *VvTUB*, was carried out before calculating fold changes. Error bar represents standard error of the mean of three biological replicates. Asterisks (\*) indicate statistically significant difference ( $P < 0.05$ ) between mock-inoculated and *B. cinerea*-inoculated samples within a post-inoculation time using unpaired heteroscedastic Student's *t* test. h.p.i., hours post-inoculation.

*cis* + *trans*-*O*-viniferin, pallidol, ampelopsin D and quadrangularin A, and *E-cis*-miyabenol; trimers: *Z*-miyabenol C and  $\alpha$ -viniferin; and the tetramer isohopeaphenol) were found highly concentrated in the infected flowers/fruitlets as compared to the control (Fig. 7a). The quantities of the stress-related *trans*- $\epsilon$ -viniferins and  $\alpha$ -viniferins, which are also involved in grapevine–*Botrytis* interaction (Langcake 1981), ranged from 0.9 to 13.4  $\mu\text{g g}^{-1}$  fresh weight (f.w.) and 2.8 to 151.8  $\mu\text{g g}^{-1}$  f.w., respectively, in the inoculated fruitlets as

compared to basal levels in the controls. A similar increase in concentration was also observed in *Z*-miyabenol C and isohopeaphenol: 1.2 to 46.4 and 0.2 to 20.9  $\mu\text{g g}^{-1}$  f.w., respectively (Supporting Information Data S9). Such an increase in the concentration of these stilbenoids suggests that they contribute to inhibiting the pathogen's advancement in colonizing the fruitlet.

In addition to STS genes, chalcone synthase (CHS) and dihydroflavonol-4-reductase (DFR), key flavonoid biosynthetic genes were DE at 24 h.p.i. (Table 2). The quantification of flavonoids revealed that flavanones, flavones, flavonols and flavan-3-ols were detected at higher concentrations following *Botrytis* inoculation, most pronouncedly at 24, 72 and 96 h.p.i. (Fig. 7a). Flavonoids are also known to restrict fungal growth and in some cases also inhibit stilbene oxidases (Goetz *et al.* 1999; Guetsky *et al.* 2005; Puhl and Treutter 2008; Nagpala *et al.* 2016).

### Infection triggers cell wall reinforcement

Reinforcing the cell wall to combat pathogen intrusion is a well-established mechanism in plants. A sign of cell wall apposition (CWA) at the site of penetration was observed by the autofluorescence of CWA regions (Fig. 8a). The enrichment analyses also proposed that the L-phenylalanine catabolic process and cell wall were among the enriched functional classes (Supporting Information Data S6). This preliminary evidence was strengthened by modulation of genes encoding cell-wall-modifying enzymes such as pectinesterases (PEs), polygalacturonases (PGs) and pectate lyases (Supporting Information Data S8). Complementary to this, we observed that genes encoding germin-like protein 3 (GLP3) and proline-rich extensin-like protein (EXT), proteins involved in  $\text{H}_2\text{O}_2$ -mediated oxidative cross-linking to toughen cell walls during pathogen attack (Bradley *et al.* 1992; Godfrey *et al.* 2007; Kelloniemi *et al.* 2015), were highly up-regulated at both 24 and 96 h.p.i. (Table 2). Grapevine genes that encode enzymes involved in monolignol biosynthesis, cinnamyl alcohol dehydrogenase and *trans*-cinnamate 4-monooxygenase were also highly up-regulated (Table 2).

Cell wall reinforcement is one of the possible mechanisms by which the grapevine flower arrests the advancement of *Botrytis*. Ten genes encoding enzymes in the monolignol biosynthesis pathway (based on the VitisNet annotations of phenylpropanoid biosynthesis) were selected for further investigation with a qPCR assay. The quantities of L-phenylalanine and seven other intermediate metabolites in this pathway were also measured by HPLC-DAD-MS (Supporting Information Data S9). Transcripts of cinnamate-4-hydroxylase (*VvC4H*) and 4-coumarate-CoA ligase (*Vv4CL*), enzymes in the upstream of the pathway, were up-regulated at the onset of *B. cinerea* infection, between 12 and 24 h.p.i., with *VvC4H* showing a peak at 12 h.p.i. (Fig. 8b). A similar trend was observed for cinnamoyl CoA reductase (*VvCCR*), the first enzyme specific to monolignol synthesis (Naoumkina *et al.* 2010). Caffeic acid *O*-methyltransferase (*VvCOMT*) and caffeoyl-CoA *O*-methyltransferase (*VvCCoAMT*) were up-regulated at 24 h.p.i. only; however, ferulate-5-hydroxylase

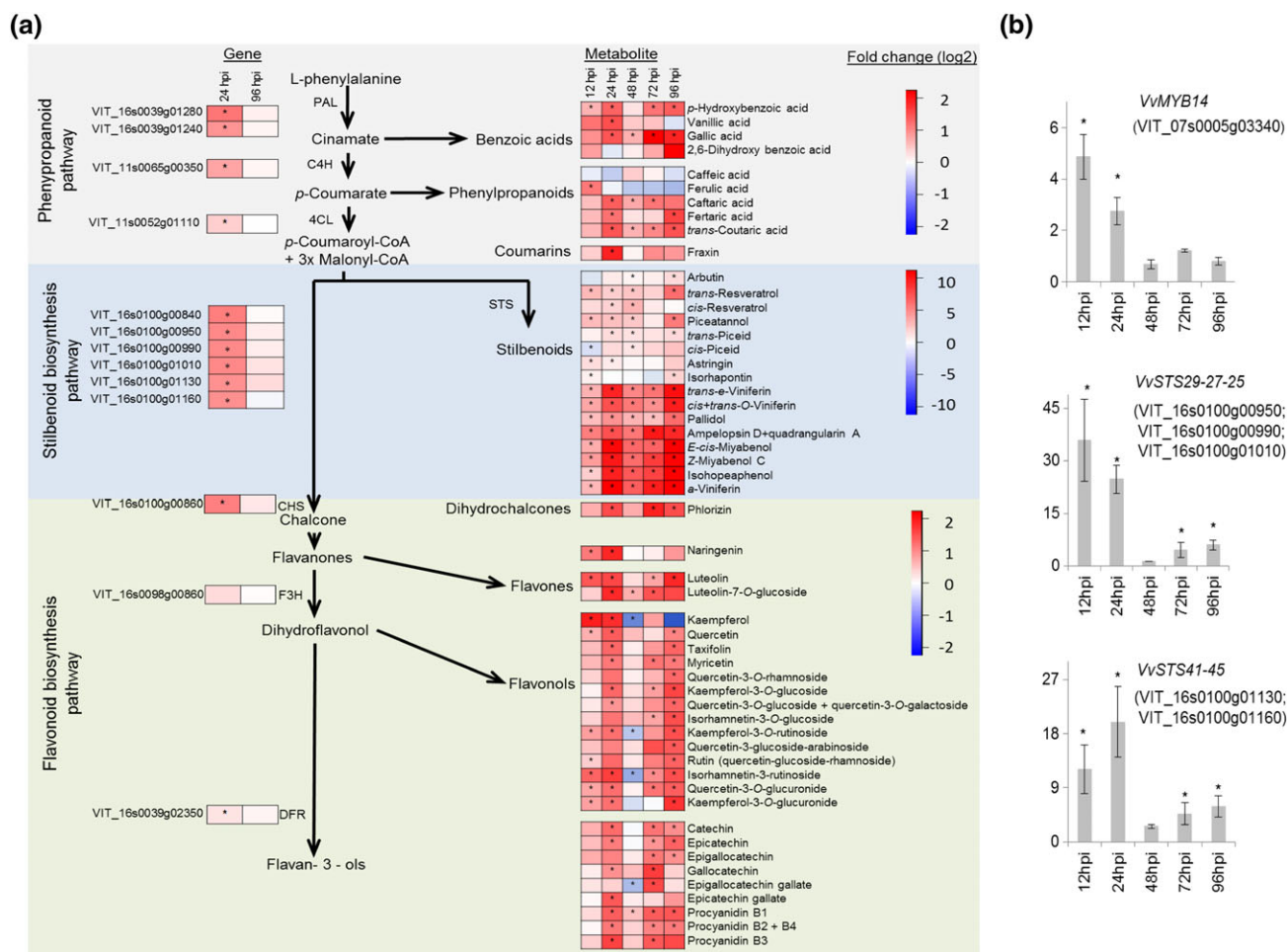


**Figure 7.** Transcript and metabolite analyses of the grapevine phenylpropanoid pathway upon *Botrytis cinerea* inoculation. (a) Heat maps of gene expression (from RNA-Seq result) and secondary metabolite concentration [ $\mu\text{g g}^{-1}$  fresh weight (f.w.)], from high-performance liquid chromatography–diode array detection–mass spectrometry (HPLC-DAD-MS) expressed as fold change. Fold changes were computed based on the ratio of average values in *B. cinerea*-inoculated and mock-inoculated flowers, for each time point. CHS, chalcone synthase; C4H, cinnamate-4-hydroxylase; 4CL, 4-coumarate-CoA ligase; DFR, dihydroflavonol-4-reductase; F3H, flavanone-3-hydroxylase; PAL, phenylalanine ammonia lyase; STS, stilbene synthase (out of 39, only six are depicted). (b) Expression profile of *VvSTS29* (-27-25), *VvSTS41* (-45) and *VvMYB14*. Gene expression levels were determined by quantitative PCR (qPCR). Bars represent fold change of inoculated sample relative to mock-inoculated sample at each post-inoculation time. Normalization based on the expression levels of actin, *VvACT*, and tubulin, *VvTUB*, was carried out before calculating fold changes. Error bar represents standard error of the mean of three biological replicates. Asterisks (\*) indicate statistically significant difference ( $P < 0.05$ ) between mock-inoculated and *B. cinerea*-inoculated samples within a post-inoculation time using unpaired heteroscedastic Student's *t* test. h.p.i., hours post-inoculation.

(*VvF5H*) was up-regulated throughout the post-inoculation time points examined. Cinnamyl alcohol dehydrogenase (*VvCAD*) was significantly up-regulated up to 48 h.p.i. In the cell wall, monolignols undergo oxidative polymerization, catalysed by peroxidases/laccases (Naoumkina *et al.* 2010). A strong up-regulation of a lignin-forming anionic peroxidase-like (*VvPER*) was observed, with the highest induction being within 24 h.p.i. (Fig. 8b). With regard to laccase, 10 genes putatively encoding laccase, having the same Kyoto Encyclopedia of Genes and Genomes (KEGG) enzyme code of *Arabidopsis* lignin laccase (Zhao *et al.* 2013), were also found extremely up-regulated, up to 90-fold (Supporting Information Data S8). Pinoresinol/lariciresinol reductase (*VvPLR*) and secoisolariciresinol dehydrogenase (*VvSIRD*)

genes, which catalyse subsequent metabolic steps to give rise to matairesinol, a lignan, as well as most of the DE genes that putatively encode dirigent-like proteins, a disease-resistance-responsive family protein involved in lignan biosynthesis, were also up-regulated in response to *B. cinerea*.

The quantification of metabolites also revealed that the concentrations of L-phenylalanine and cinnamate, which represent the two key entry substrates in the monolignol biosynthesis pathway, were significantly higher in *Botrytis*-inoculated flowers (Fig. 8c). In contrast, the concentrations of *p*-coumarate, caffeate, ferulate and 5-hydroxyferulate were not different between *Botrytis*-inoculated flowers and control samples, probably because of their rapid conversion into the next metabolite of the pathway. Exceptions were the two

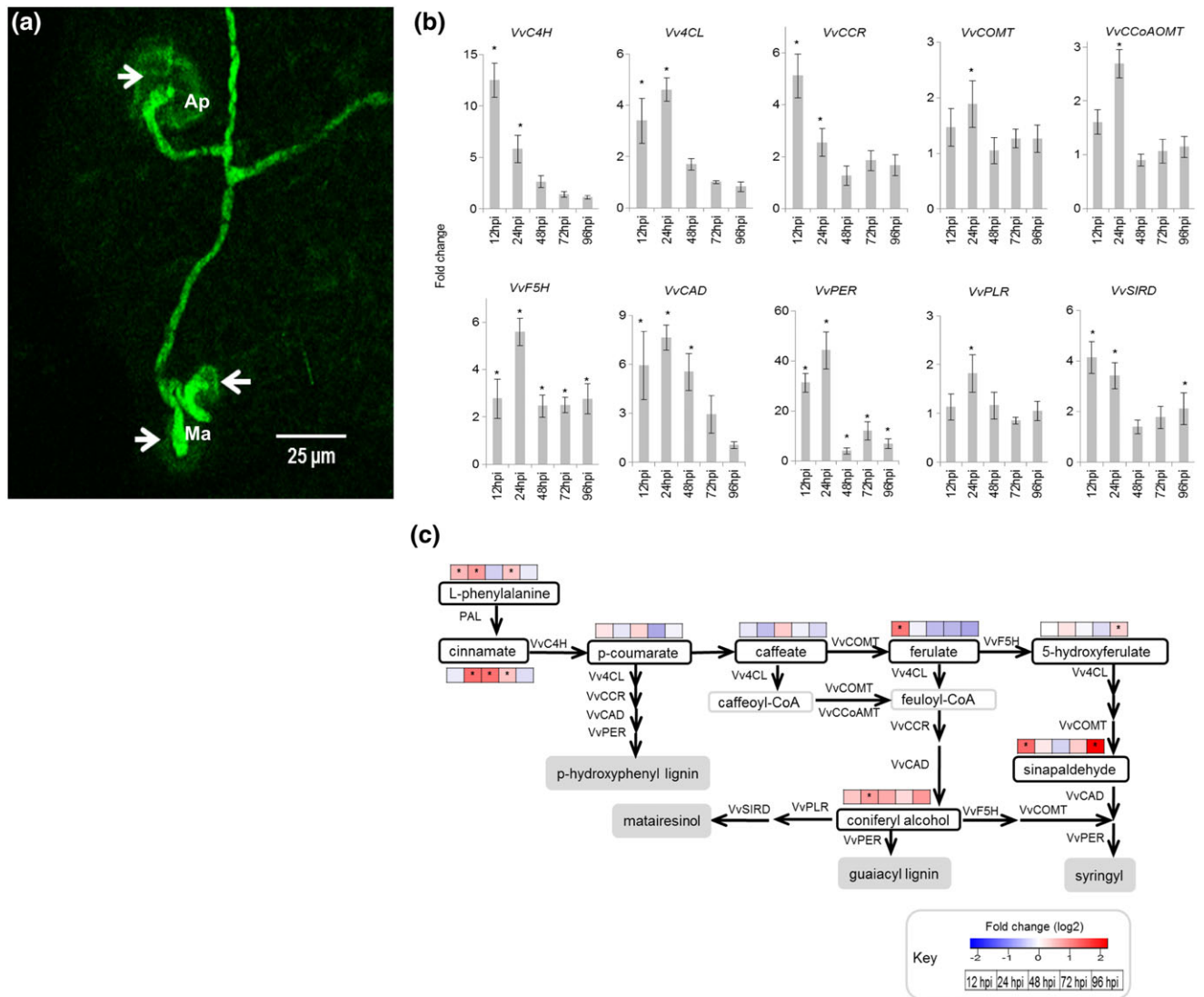


**Figure 8.** Cell wall apposition and monolignol biosynthesis pathway in *Botrytis cinerea*-infected flowers. (a) Confocal microscope image at 30 h.p.i. of GFP-labelled *B. cinerea*. Autofluorescence around penetration site (shown by arrow) indicates cell wall apposition. Ap, appressoria; and Ma, multicellular appressoria (infection cushions). (b) Expression profile of genes encoding key enzymes of the grapevine monolignol biosynthetic pathway. *VvCAD*, cinnamyl alcohol dehydrogenase; *VvCOMT*, caffeic acid *O*-methyltransferase; *VvCCoAMT*, caffeoyl-CoA *O*-methyltransferase; *VvC4H*, cinnamate-4-hydroxylase; *VvCCR*, cinnamoyl CoA reductase; *Vv4CL*, 4-coumarate-CoA ligase; *VvF5H*, ferulate 5-hydroxylase; *PAL*, phenylalanine ammonia lyase; *VvPER*, peroxidase (lignin-forming anionic peroxidase-like); *VvPLR*, pinoresinol/lariciresinol reductase; *VvSIRD*, secoisolariciresinol dehydrogenase. Gene expression levels were determined by quantitative PCR (qPCR). Bars represent fold change of *B. cinerea*-inoculated sample relative to mock-inoculated sample at each post-inoculation time. Normalization based on the expression levels of actin, *VvACT*, and tubulin, *VvTUB*, was carried out before calculating fold changes. Error bar represents standard error of the mean of three biological replicates. (c) Heat map of monolignol precursors superimposed to the biosynthetic pathway. The amounts of monolignol precursors [ $\mu\text{g g}^{-1}$  fresh weight (f.w.)] were quantified by high-performance liquid chromatography–diode array detection–mass spectrometry (HPLC-DAD-MS). Fold changes were computed based on the ratio of average values of *B. cinerea*-inoculated and mock-inoculated flowers, for each time point. Monolignol and lignan compounds are highlighted in grey background. Asterisks (\*) indicate statistically significant difference ( $P < 0.05$ ) between mock-inoculated and *B. cinerea*-inoculated samples within a post-inoculation time using unpaired heteroscedastic Student's *t* test.

intermediates, sinapaldehyde and coniferyl alcohol, metabolites found towards the end of the pathway, which were generally higher in the *Botrytis*-inoculated flowers than in the control samples.

These results indicate that upon *B. cinerea* infection, cell wall fortification was among the defence mechanisms employed by the flowers/fruitlets to contain the pathogen in its quiescent state.

### *Botrytis cinerea* transcripts expressed in planta during grapevine flower infection

The signal of *B. cinerea* transcripts detected in inoculated flowers was very low (Supporting Information Data S2 and S10). Therefore, it was not possible to perform a statistical comparison between the transcriptome of the infecting pathogen versus the PDB-grown fungus, and an alternative

approach was applied. Genes from *B. cinerea* were considered expressed if they were represented by an average of at least 10 reads in the three biological replicates of inoculated flower samples. A total of 1325 genes met these conditions and will be herein referred to as ‘*in planta* expressed genes’. Of these 1325 genes, 751 and 59 were expressed only at 24 and 96 h.p.i., respectively, and 515 genes were expressed at both 24 and 96 h.p.i. (Supporting Information Data S11).

Some of the *in planta* expressed genes exhibited high raw reads as compared to the others, but majority of them are annotated as predicted/hypothetical proteins and ribosomal or housekeeping proteins. Other genes worth to mention because of being possibly involved in plant–fungus interaction are *Bcin12g01020* and *Bcin14g00850*, encoding oxaloacetate and polygalacturonase, respectively; *Bcin03g00640* and *Bcin13g05810*, encoding putative alcohol oxidase and aldehyde dehydrogenase, respectively; *Bcin06g03370* encoding putative 4-dehydrocholesterol reductase precursor/mitochondrial phosphate carrier 2; *Bcin05g04530*, encoding putative ET receptor/hsp90; and *Bcin02g07470* encoding putative byssal cuticle protein. In mussels, byssal cuticle facilitates its attachment to a substrate (Waite *et al.* 1989; Lee *et al.* 2011). The protein may also have a role in facilitating *Botrytis* attachment to the plant surface; its raw reads were higher at 24 h.p.i. than at 96 h.p.i. but had almost no expression in PDB culture (Supporting Information Data S11).

The set of *in planta* expressed genes were functionally annotated using Blast2GO (Conesa *et al.* 2005) and Amselem *et al.* (2011) (Supporting Information Data S11). The joined biological meaning of the genes was visualized using the Combined Graph Function of Blast2GO based on their GO slim terms, and primary metabolic process, nitrogen compound metabolic process, ion binding, oxidoreductase activity and

cytoplasmic component were among the most represented GO terms (Supporting Information Data S12). The most important functional categories associated to the expressed genes are reported in Table 3. *In planta* expressed genes encompassed genes involved in pathogenesis, such as carbohydrate-active enzymes (CAZymes) devoted to plant cell wall degradation, in ROS production and detoxification, in toxin biosynthesis and in transcriptional regulation; all these genes were more abundant at 24 h.p.i. Besides, many ribosomal and histone genes were equally abundant at 24 and 96 h.p.i., indicating the maintenance of a basal metabolism during quiescence.

### **Botrytis cinerea genes required for pathogenesis are up-regulated during flower infection**

A group of 23 *in planta* expressed genes known to be related to *Botrytis* growth or pathogenesis were further characterized by qPCR. In addition, two other genes, GST (*BcGST1*) and polygalacturonase 2 (*BcPG2*), were analysed. qPCR expression profiles are shown in Fig. 9, while gene names together with the expression level from the RNA-Seq analysis are reported in Table 4.

All genes showed a sharp peak of expression at 24 h.p.i., except superoxide dismutase 1 (*BcSOD1*), *BcGST1* and the constitutively expressed *BcPG1*. Genes such as oxaloacetate acetyl hydrolase (*BcOAH*), cutinase (*BcCUT-like1*) and pectate lyase (*BcPEL-like1*) appeared to be expressed exclusively during a *Botrytis* attack, while other genes were also expressed in the absence of the host, but much more so during the host–pathogen interaction.

*Botrytis cinerea* cutinases *BcCUTA* and *BcCUT-like1* are involved in the breaching of the cuticle layer by appressoria.

**Table 3.** Specific functions of *in planta* detected *Botrytis cinerea* transcripts

Functions of <i>B. cinerea</i> genes	No. of genes involved	
	24 h.p.i.	96 h.p.i.
Proteins identified as early secretome, within 16 h of germination (Espino <i>et al.</i> 2010)	39	9
Carbohydrate-active enzymes (CAZymes) (Amselem <i>et al.</i> 2011; Blanco-Ulate <i>et al.</i> 2014)	203	64
CAZymes acting on fungal cell wall	36	16
CAZymes acting on plant cell wall	56	11
CAZymes acting on cellulose	5	2
CAZymes acting on hemicellulose	20	3
CAZymes acting on hemicellulose and pectin side chains	9	0
CAZymes acting on pectin	23	1
Proteins generating reactive oxygen species (ROS) (Schumacher <i>et al.</i> 2014)	10	2
Proteins involved in the detoxification of ROS (Schumacher <i>et al.</i> 2014)	23	8
Protease (Amselem <i>et al.</i> 2011)	38	8
Secondary metabolism key enzymes (Amselem <i>et al.</i> 2011)	3	0
60S and 40S ribosomal proteins (Amselem <i>et al.</i> 2011)	78	78
Appressorium-associated genes (orthologs in <i>Magnaporthe oryzae</i> ) (Amselem <i>et al.</i> 2011)	7	2
Transporters	64	22
Transcription factors	29	13
Histone	8	7
Actin	11	6

This invasive step normally causes oxidative burst in the host (Schouten *et al.* 2002a), which is counteracted by the activation of scavenging mechanisms in the pathogen. The transcription levels of several *B. cinerea* genes taking part in the ROS-mediated fungus–plant interaction were quantified (Fig. 9a). *BcSOD1*, which plays a role in oxidative stress response during cuticle penetration (Rolke *et al.* 2004); H<sub>2</sub>O<sub>2</sub> generators galactose oxidase (*BcGOX1*) and alcohol oxidase (*BcAOX*); ROS scavengers *BcGST*, peroxidase 1 (*BcPRD1*) and glutathione peroxidase (*BcGPX3*) (Schumacher *et al.* 2014);

and *BcLCC2*, a gene involved in the oxidation of resveratrol and tannins (Schouten *et al.* 2002b), were all involved in the *Botrytis*–grapevine interaction.

A similar expression profile, albeit quantitatively different, was shown by CWDEs (Fig. 9b). *PG*, pectate lyase (*BcPEL-like1*) and oxaloacetate acetyl hydrolase (*BcOAH*) are involved in pectin degradation. Galacturonate reductase (*BcGAR2*), galactonate dehydratase (*BcLGD1*) and 2-keto-3-deoxy-L-galactonate aldolase (*BcLGA1*), genes that play a role in the catabolic pathway of D-galacturonic acid (Zhang

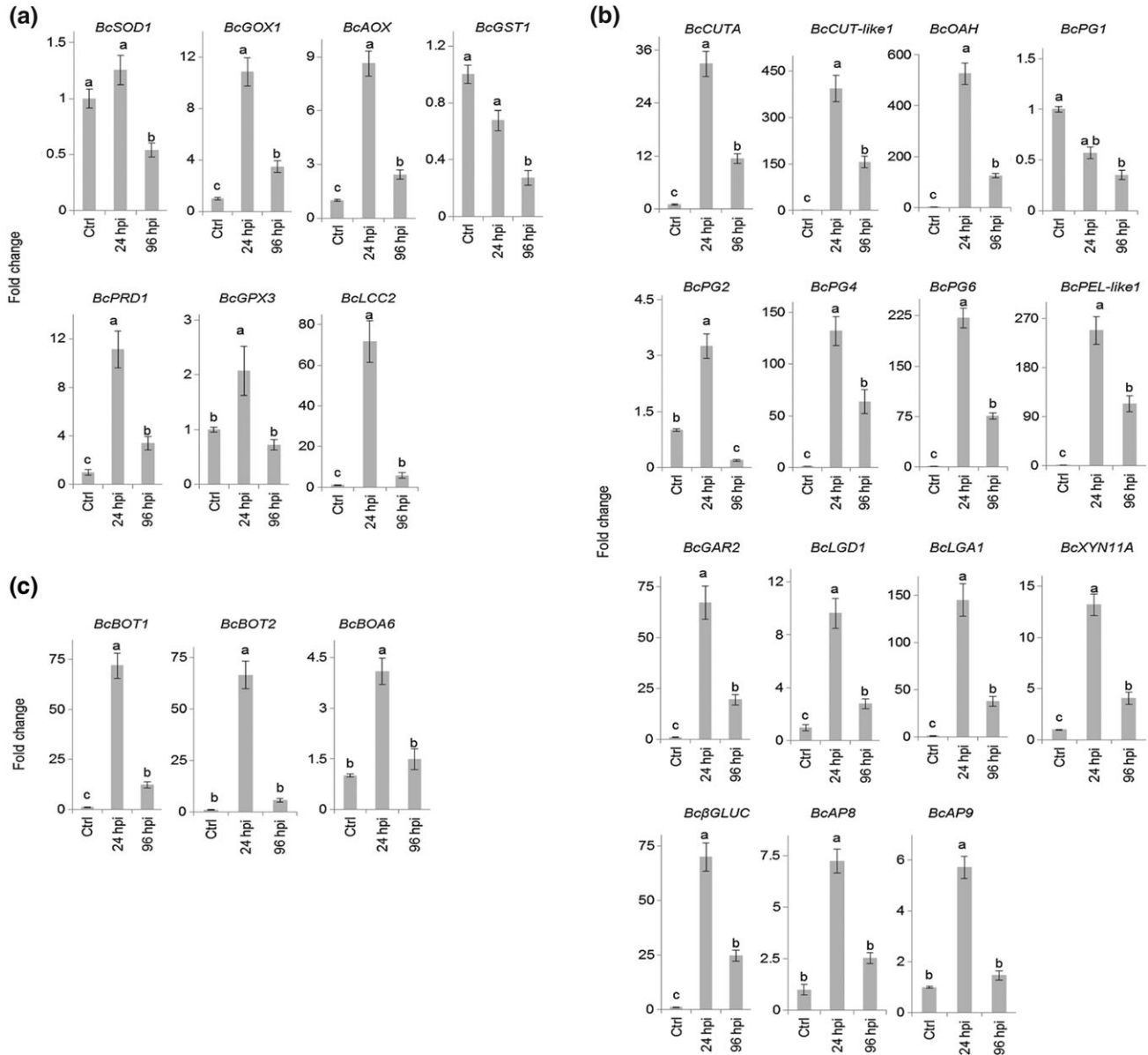


**Figure 9.** Expression profile of growth-related and virulence-related *Botrytis cinerea* genes during grapevine flower infection [at 24 and 96 hours post-inoculation (h.p.i.) relative to potato dextrose broth (PDB)-cultured *B. cinerea*]. (a) Reduction–oxidation-related genes. (b) Cell-wall-degrading enzymes and protease encoding genes. (c) Phytotoxin encoding genes. Gene expression levels were determined by quantitative PCR (qPCR). Bars represent fold change of sample at 24 or 96 h.p.i. relative to the PDB-cultured *B. cinerea* (Ctrl). Normalization based on the expression levels of ribosomal protein L5, *BcRPL5*, and  $\alpha$ -tubulin, *BcTUBA*, was carried out before calculating fold changes. Error bar represents standard error of the mean of three biological replicates. Expression values followed by a common letter are significantly not different between samples, according to Tukey's honestly significant difference test ( $P \leq 0.05$ ), using one-way ANOVA of  $\log_2(\text{NRQ})$ .

**Table 4.** RNA-Seq reads of *B. cinerea* transcripts checked by qPCR assay

Abbreviation	Transcript description	Gene ID	Average no. of raw reads from RNA-Seq analysis			
			<i>In planta</i> expressed		PDB culture	
			24 h.p.i.	96 h.p.i.		
<i>BcSOD1</i>	Superoxide dismutase 1	Bcin03g03390	76	26	9411 <sup>a</sup>	
<i>BcGOX1</i>	Galactose oxidase	Bcin13g05710	21		609	
<i>BcAOX</i>	Alcohol oxidase	Bcin07g03040	24		490	
<i>BcGST1</i>	Glutathione S-transferase	Bcin10g00740			2655 <sup>a</sup>	
<i>BcPRD1</i>	Dyp-type peroxidase	Bcin13g05720	19		312	
<i>BcGPX3</i>	Glutathione peroxidase	Bcin03g01480	23		2871 <sup>a</sup>	
<i>BcLCC</i>	Laccase 2	Bcin14g02510	15		32 <sup>b</sup>	
<i>BcCUTA</i>	Cutinase	Bcin15g03080	15		54 <sup>b</sup>	
<i>BcCUT-likel</i>	Cutinase	Bcin01g09430	68	11	9 <sup>b</sup>	
<i>BcOAH</i>	Oxaloacetate acetyl hydrolase	Bcin12g01020	386		38 <sup>b</sup>	
<i>BcPG1</i>	Polygalacturonase 1	Bcin14g00850	209	175	147 821 <sup>a</sup>	
<i>BcPG2</i>	Polygalacturonase 2	Bcin14g00610			362	
<i>BcPG4</i>	Polygalacturonase 4	Bcin03g01680	44		47 <sup>b</sup>	
<i>BcPG6</i>	Polygalacturonase 6	Bcin02g05860	75		62	
<i>BcPEL-likel</i>	Pectate lyase	Bcin03g05820	87	24	40 <sup>b</sup>	
<i>BcGAR2</i>	D-Galacturonic acid reductase 2	Bcin03g01500	37		104	
<i>BcLGD1</i>	D-Galactonate dehydrogenase	Bcin01g09450	61	10	804	
<i>BcLGA1</i>	2-Keto-3-deoxy-L-galactonate aldolase	Bcin03g01490	70	13	66	
<i>BcXYN1IA</i>	Endo- $\beta$ -1,4-xylanase	Bcin03g00480	18		129	
<i>Bc<math>\beta</math>GLUC</i>	Beta-glucosidase 1 precursor	Bcin10g05590	32		75	
<i>BcAP8</i>	Aspartic proteinase 8	Bcin12g02040	30	12	1064 <sup>a</sup>	
<i>BcAP9</i>	Aspartic proteinase 9	Bcin12g00180	16		569	
<i>BcBOT1</i>	Botrydial biosynthesis 1	Bcin12g06380	58		86	
<i>BcBOT2</i>	Botrydial biosynthesis 2	Bcin12g06390	41		55	
<i>BcBOA6</i>	Botcinic acid 6	Bcin01g00060	13		1048 <sup>a</sup>	

<sup>a</sup>Transcripts whose average raw reads are in the top 25%, most expressed, in PDB culture.

<sup>b</sup>Transcripts whose average reads are in the bottom 25%, least expressed, in PDB culture.

*et al.* 2011), a major component of pectin polysaccharides (Mohnen 2008; Caffall and Mohnen 2009), also had similar trends of expression. The strong and similar expression pattern in pectin and D-galacturonic-acid-degrading enzymes suggested that the degradation of the pectin backbone was initiated at 24 h.p.i. The involvement of other CWDEs, such as endo- $\beta$ -1,4-xylanase (*BcXYN1IA*), which degrades hemicellulose and also induces necrosis (Noda *et al.* 2010);  $\beta$ -glucosidase (*Bc $\beta$ GLUC*), which degrades both cellulose and hemicellulose (Gilbert 2010; Blanco-Ulate *et al.* 2014); and secreted aspartic proteinases (*AP*), was also highlighted from the qPCR assay (Fig. 9b). The RNA-Seq data further suggested the involvement of pectin lyases (Bcin03g00280 and Bcin03g07360), enzyme acting preferentially on highly methyl esterified pectin, in the infection process (Supporting Information Data S11).

The strong up-regulation of botcinic acid (*BcBOA*) and botrydial phytotoxins (*BcBOT*) genes, involved in phytotoxin synthesis, pointed towards their participation in the fungal infection programme (Fig. 9c).

Taken together, these results indicate the readiness of the fungus to colonize the flowers within 24 h.p.i. However, the transcript levels of all of the tested infection-related *B. cinerea* genes were much lower at 96 h.p.i., suggesting that the pathogenesis programme initiated at 24 h.p.i. is halted at a later time point. The transcriptional profile of *BcACTA* also

suggested that the activity of the fungus decreased towards the later hours of infection. From the post-inoculation inspection of the infected flowers, no visible disease progress was detected until ripening (Fig. 1). This strengthens the hypothesis that the fungus reduced its biological activity and entered into a quiescent phase.

## DISCUSSION

In grapevine, the epidemiology of the fungus, especially the infection process of the pathogen during flowering, is largely unknown. *B. cinerea* infection of grapevine inflorescence at blooming followed by a 'latency period' was first reported by McClellan and Hewitt (1973). This observation was further confirmed by Keller *et al.* (2003) where inoculation at full bloom caused high disease severity at harvest. Using the advantage of a GFP-labelled B05.10 strain, we could show for the first time that *B. cinerea* inoculated at the flower cap-off stage remained in a quiescent state until berry full coloration (for about 2.5 months), and then it resumed active growth and invaded the berries when the microclimate was conducive (high humidity). This study provides a detailed description of the infection processes from infection initiation (24 h.p.i.) to initial fungal quiescent (96 h.p.i.) stages by means of transcriptomic and metabolic analyses and microscopic

observations, laying the foundation for understanding the mechanism of the plant–fungus interaction during flowering, which leads to pathogen quiescence.

Following the GFP fluorescence signal of the *Botrytis*, there was penetration of the fungus into the flower cuticle within 24 h.p.i. but no further appreciated growth at 96 h.p.i. Confocal microscopy and transcriptomic studies showed that the fungus attempted to establish infection on grapevine flowers before becoming quiescent as observed from the germinated appressoria in the flower gynoecium (Fig. 1b,g) and a prevalent modulation of defence-related genes within 24 h.p.i. The main functional categories of the *in planta* expressed genes of the fungus were those related to pathogenesis (Table 3). The conidia germination event of *B. cinerea* is accompanied by a rapid shift in gene expression, for both germ tube outgrowth and host cell invasion (Leroch *et al.* 2013). Interestingly, much of these *in planta* expressed genes were also differentially regulated during successful infection of ripe grapevine berries (16, 24 and 48 h.p.i.) (Kelloniemi *et al.* 2015), *Lactuca sativa* (12, 24 and 48 h.p.i.) (De Cremer *et al.* 2013) and *Solanum lycopersicoides* (24 and 48 h.p.i.) (Smith *et al.* 2014). This suggests that the *in planta* expressed genes were part of the pathogenesis mechanisms deployed in grapevine flowers that would help to establish infection.

One of the key processes in establishing infection by *B. cinerea* is the depolymerization of cell wall components (van Kan 2006; Williamson *et al.* 2007; Zhang *et al.* 2011). Generally, after breaching the cuticular layer of host tissues, *B. cinerea* often grows into the pectin-rich anticlinal wall of the underlying epidermal cell (van Kan 2006; Williamson *et al.* 2007), by the activation of pectinases. In our study, almost all of the assayed CWDEs were expressed at a higher level at 24 h.p.i. (Fig. 9). Besides increased levels of CWDEs, the up-regulation of genes encoding the biosynthesis of phytotoxic secondary metabolites and secreted proteases, which assist the infection process (Dalmais *et al.* 2011; Rossi *et al.* 2011), further confirmed that the fungus put in place several strategies to invade the grapevine flowers. Nonetheless, there was no visible disease symptoms observed in the post-inoculation observations despite the presence of *B. cinerea* confirmed by the plating-out experiment (Fig. 1h). The much lower number of *Botrytis* genes expressed *in planta* at 96 h.p.i. as compared to 24 h.p.i. (65% less), as well as the estimated ratio of *B. cinerea* to grapevine RNA (1:500, Supporting Information Data S2) compared to the much smaller ratio for genomic DNA (about 1:20, Fig. 1i) in the same tissue, is also a confirmation that the fungus entered the quiescent phase.

Quiescence of a pathogen can happen before conidia germination, at the initial hyphal development stage, before or after appressorium formation, after appressorium germination and/or at the subcuticular hyphae stage (Prusky 1996). In unripe tomato, *Colletotrichum gloeosporioides* becomes quiescent as a swollen hyphae after appressorium germination (Alkan *et al.* 2015), whereas *Alternaria alternata* enters into quiescence after its hypha penetrates the cuticular layer of young apricot, persimmon and mango fruits (Prusky 1996). For *B. cinerea*, cell-wall-penetrated hypha was proposed as a quiescent stage of infection in immature grape berries (Keller *et al.* 2003). Although the quiescence of ungerminated

conidia cannot be completely ruled out in our case, the microscopic observation of conidia germination and appressorium formation (Fig. 1g and Supporting Information Fig. S4), together with the results of the plating-out experiment, which showed a non-significant effect of washing the inoculated berries (Fig. 1h), indicates that the pathogen entered into a quiescent state after penetrating the cell wall. The burst of defence-related reactions from the plant is also an indirect support of this claim.

In our study, the attempted infection by *B. cinerea* instigated a multilayered defence response in the grapevine flower tissues. Following inoculation, more than 70 RLKs were DE within 24 h.p.i. (Supporting Information Data S8). Several of these RLKs have been described to be involved in immune response to pathogens. The perception of cell wall fragments, such as oligogalacturonides (OGs) due to CWDE, induces basal resistance to the pathogen (Boller and Felix 2009). In *Arabidopsis thaliana*, overexpressing the OG receptor *WAK1* enhanced resistance to *B. cinerea* (Brutus *et al.* 2010) but on the other hand increased susceptibility to *Sclerotinia sclerotiorum*, and *B. cinerea* was observed in BAK1 mutant *Arabidopsis* (Kemmerling *et al.* 2007; Zhang *et al.* 2013). The RLK BAK1 constitutes a negative control element of microbial-infection-induced cell death in plants (Kemmerling *et al.* 2007). These two RLKs exhibited increased expression levels in powdery-mildew-resistant *Vitis pseudoreticulata* in response to *E. necator* (Weng *et al.* 2014) and in *B. cinerea*-challenged lettuce (De Cremer *et al.* 2013). We also saw up-regulation of genes coding for these membrane receptor proteins at 24 h.p.i., indicating that the plant recognized the pathogen and triggered immunity responses: quick and strong induction of PR proteins and accumulation of stress-related secondary metabolites, as well as cell wall lignification, were deployed as major defence responses to halt the infection. The oxidative stress caused during the interaction seemed mainly managed by GSTs and ascorbate oxidases (Marrs 1996) as more than 20 genes coding for them were up-regulated at 24 h.p.i. The pathogen-responsive *PR10*, *PR5* (thaumatin-like protein) and chitinases also had a marked up-regulation (between fivefold and 40-fold up-regulation within 24 h.p.i.). *PR5* and chitinases are known for their inhibition of fungal growth including *B. cinerea* (Giannakis *et al.* 1998; Monteiro *et al.* 2003). From our qPCR result, a coordinated expression of *VvWRKY33*, *VvPR10.1* and *VvPR10.3* was demonstrated. *VvPR10.1* was recently associated to *P. viticola* resistance, in grapevine under the regulation of *VvWRKY33* (Merz *et al.* 2015). Even though the two pathogens are biologically different and may not necessarily activate a similar response from their hosts, *VvPR10.1* and *VvPR10.3*, a PR belonging to the same group of *VvPR10.1* (Lebel *et al.* 2010), had the highest up-regulation among the expressed PRs, making them strong candidates for the resistance of grapevine flower to *B. cinerea*. In *Arabidopsis* *WRKY33*, the functional homolog of *VvWRKY33* (Merz *et al.* 2015) plays a key role in the plant defence process, regulating redox homeostasis, SA signalling, ET–JA-mediated cross-communication and phytoalexin biosynthesis conferring resistance to *B. cinerea* (Birkenbihl *et al.* 2012).



Upon *B. cinerea* infection, grapevine berries activate stilbenoid biosynthesis (Langcake 1981; Jeandet *et al.* 1995; Keller *et al.* 2003; Agudelo-Romero *et al.* 2015; Kelloniemi *et al.* 2015). Our results were in line with previous evidence. From the RNA-Seq results, it seemed that the genes coding for STS and laccase proteins were switched on following the infection, as most of them were below the detection limit in the mock-inoculated flowers. The activation of the polyphenol biosynthetic pathway was further investigated by a more fine-grained expression profile of the transcription factor regulating stilbene biosynthesis (*VvMYB14*, Höll *et al.* 2013) together with *VvSTS29* and *VvSTS41* and by measuring the concentration of several classes of polyphenols (phenylpropanoids, stilbenoids and flavonoids). The phytoalexin resveratrol, which inhibits *B. cinerea* growth (Schouten *et al.* 2002b; Favaron *et al.* 2009), and its monomeric and oligomeric derivatives, some with documented antifungal activity (Hammerbacher *et al.* 2011), were all up-regulated starting from 12 h.p.i. The concentrations of  $\epsilon$ -viniferin and  $\alpha$ -viniferin, dimer and trimer resveratrol, respectively, were higher in *Botrytis*-infected flowers than in control. These compounds represent the predominant stress metabolites in Vitaceae–*B. cinerea* interactions (Langcake 1981). We also observed a marked oligomerization of resveratrol to ampelopsin D and quadrangularin, *E*-*cis*-miyabenol, *Z*-miyabenol C and isohopeaphenol upon infection, which agrees with the hypothesis that oligomerization of resveratrol leads to more toxic compounds (Pezet *et al.* 2003a). On the other hand, the glycosylated form of resveratrol, *trans*-piceid, was also shown to involve in *Colletotrichum higginsianum* resistance in *Arabidopsis* (Liu *et al.* 2011). A strong correlation was also observed between the concentration of stilbenic phytoalexins and resistance to *P. viticola* in both a *Vitis riparia* and *Merzling*  $\times$  *Teroldego* cross-population (Langcake 1981; Malacarne *et al.* 2011).

The potent stilbene oxidase inhibitors caftaric and *trans*-coutaric acids (both phenylpropanoids), catechin and quercetin-3-*O*-glucuronide (both flavonoids) (Goetz *et al.* 1999) were also detected at higher concentrations in the *Botrytis*-infected flowers than in the control. These compounds possibly interfered with the fungal laccase activity by inactivating its oxidizing and insolubilizing effects on stilbenic phytoalexins and PR proteins (Goetz *et al.* 1999; Favaron *et al.* 2009). In addition, different classes of flavonoids including proanthocyanidins (procyanidins B1, B2, B3 and B4) were also detected at a higher concentration in the infected flowers; these compounds can act as inhibitors of enzymes such as polygalacturonases. A higher concentration of proanthocyanidins in the epidermal layer of immature strawberry, at the periphery of *B. cinerea* penetration, was reported to restrict further growth of *B. cinerea* and keep the pathogen under quiescence (Jersch *et al.* 1989). Taken together, our results indicated a dramatic and rapid accumulation of the polyphenolic metabolites, in particular stilbenoids, at the site of infection, suggesting this is a mechanism of defence to induce *B. cinerea* quiescence in grapevine flower.

Reinforcing cell walls is another strategy of plant resistance against pathogens. From our microscopic observations, CWA

occurred at the appressorium penetration site (Figs 1f and 8a). Gene expression and metabolite analysis also indicated that grapevine flowers, upon *B. cinerea* infection, activated the monolignol biosynthesis pathway within 24 h.p.i. A similar phenomenon occurs in wheat, where up-regulation of monolignol genes within 24 h.p.i. conferred resistance to *Blumeria graminis* f. sp. *tritici*; and silencing a few key genes in the pathway (*PAL*, *COMT*, *CCoAMT* and *CAD*) compromised penetration resistance of the plant to the pathogen (Bhuiyan *et al.* 2009). The up-regulation of *GLP3* and *EXT*, both at 24 and 96 h.p.i., and accumulation of H<sub>2</sub>O<sub>2</sub> around the penetration site, as shown using the HyPer signal (Fig. 5), suggest CWA was triggered as an early response to the infection. H<sub>2</sub>O<sub>2</sub>-mediated oxidative cross-linking and lignin synthesis to reinforce CWA and halt *B. cinerea* infection were recently shown in grapevine by Kelloniemi *et al.* (2015). In their study, the up-regulation of lignin-forming enzymes (*GLP3* and *EXT*) together with the accumulation of H<sub>2</sub>O<sub>2</sub>, at the site of *Botrytis* penetration, was part of the defence mechanisms used by the veraison berry to arrest the pathogen. However, no such queues of responses were seen in the mature berry where the pathogen readily managed to colonize the berry tissue (Kelloniemi *et al.* 2015). In green tomatoes, usually resistant to *B. cinerea*, the accumulation of H<sub>2</sub>O<sub>2</sub> and lignin occurs at the site of inoculation (Cantu *et al.* 2009), and in a tomato *sitiens* mutant, primed H<sub>2</sub>O<sub>2</sub> accumulation and cell wall reinforcement were among the resistant factors against *B. cinerea* (Asselbergh *et al.* 2007). These all show that the CWA-mediated resistance was also active in the *B. cinerea*-infected flowers.

The ability of grape berries in keeping the pathogen under quiescence is however broken at ripening (Supporting Information Fig. S6). This study was not designed to pinpoint the berry signals that trigger a pathogen's transition from the prolonged quiescent to egression state. However, the changes in physical and chemical properties occurring at ripening, such as activation of phytohormone biosynthesis, cuticular changes, cell wall loosening, conversion of acids into sugars and a steadily diminishing of antifungal compounds (both pre-formed and inducible secondary metabolites), are likely to favour pathogen egression (Prusky 1996; Prusky *et al.* 2013). Another factor that may modulate the transition from a quiescent to necrotrophic state is the production of host signals, such as ET, which can trigger fungal pathogenicity factors (Prusky 1996). Alongside the decline in resistance during ripening (Pezet *et al.* 2003b; Prusky and Lichter 2007), the sugar and organic acid exudates appearing on the berry surface during ripening (Padgett and Morrison 1990; Kretschmer *et al.* 2007) likely stimulate and promote *B. cinerea* outgrowth. In conclusion, the higher expression level of *B. cinerea* genes encoding for CWDE, phytotoxic secondary metabolites and proteases within 24 h.p.i. upon contact with the grapevine flower indicated a readiness to establish a successful infection. However, there was no visible disease symptom for about 12 weeks, until the egression was apparent at the ripening stage. Flowers reacted readily to the infection as their defence mechanisms were very in-line upon recognizing the intruder. There was a marked accumulation of

antimicrobial proteins (mainly PR proteins), monolignol precursors, stilbenoids and ROS accompanied by cell wall reinforcement. The conjugated actions of these induced defence responses seem to be responsible for forcing *B. cinerea* into quiescence until more favourable conditions occur in the berry.

## ACKNOWLEDGMENTS

The research was funded by the Autonomous Province of Trento (PAT-ADP 2013–2016). Z.M.H. is a recipient of a FIRST scholarship from FEM. The authors would like to thank Dr Domenico Masuero (FEM) for the support with biochemical analysis, Dr Alex Costa (University of Milan) for provision of the HyPer construct, Dr Daniele Brazzale (FEM) for his technical assistance, Dr Ulrike Siegmund and Dr Julia Schumacher (University of Muenster) for the help with microscopy and for provision of the GFP-labelled B05.10 strain of *B. cinerea*, Dr Umberto Salvagnin (FEM) for taking of the pictures of the grapevine plants and Dr Giovanna Flaim for the English revision of the manuscript.

## REFERENCES

- Agudelo-Romero P., Erban A., Rego C., Carbonell-Bejerano P., Nascimento T., Sousa L., ... Fortes A.M. (2015) Transcriptome and metabolome reprogramming in *Vitis vinifera* cv. Trincadeira berries upon infection with *Botrytis cinerea*. *Journal of Experimental Botany* **66**, 1769–1785.
- Alkan N., Friedlander G., Ment D., Prusky D. & Fluhr R. (2015) Simultaneous transcriptome analysis of *Colletotrichum gloeosporioides* and tomato fruit pathosystem reveals novel fungal pathogenicity and fruit defense strategies. *New Phytologist* **205**, 801–815.
- Anselm J., Cuomo C.A., van Kan J.A., Viaud M., Benito E.P., Couloux A., ... Dickman M. (2011) Genomic analysis of the necrotrophic fungal pathogens *Sclerotinia sclerotiorum* and *Botrytis cinerea*. *PLoS Genetics* **7**, e1002230.
- Asselbergh B., Curvers K., Franca S.C., Audenaert K., Vuylsteke M., Van Breusegem F. & Höfte M. (2007) Resistance to *Botrytis cinerea* in sitiens, an abscisic acid-deficient tomato mutant, involves timely production of hydrogen peroxide and cell wall modifications in the epidermis. *Plant Physiology* **144**, 1863–1877.
- Bhuiyan N.H., Selvaraj G., Wei Y. & King J. (2009) Role of lignification in plant defense. *Plant Signaling & Behavior* **4**, 158–159.
- Birkenbihl R.P., Diezel C. & Somssich I.E. (2012) *Arabidopsis* WRKY33 is a key transcriptional regulator of hormonal and metabolic responses toward *Botrytis cinerea* infection. *Plant Physiology* **159**, 266–285.
- Blanco-Ulate B., Morales-Cruz A., Amrine K.C., Labavitch J.M., Powell A.L. & Cantu D. (2014) Genome-wide transcriptional profiling of *Botrytis cinerea* genes targeting plant cell walls during infections of different hosts. *Frontiers in Plant Science* **5**, 435.
- Boller T. & Felix G. (2009) A renaissance of elicitors: perception of microbe-associated molecular patterns and danger signals by pattern-recognition receptors. *Annual Review of Plant Biology* **60**, 379–406.
- Bradley D.J., Kjellbom P. & Lamb C.J. (1992) Elicitor- and wound-induced oxidative cross-linking of a proline-rich plant cell wall protein: a novel, rapid defense response. *Cell* **70**, 21–30.
- Brutus A., Sicilia F., Macone A., Cervone F. & De Lorenzo G. (2010) A domain swap approach reveals a role of the plant wall-associated kinase 1 (WAK1) as a receptor of oligogalacturonides. *Proceedings of the National Academy of Sciences, USA* **107**, 9452–9457.
- Caffall K.H. & Mohnen D.B. (2009) The structure, function, and biosynthesis of plant cell wall pectic polysaccharides. *Carbohydrate Research* **344**, 1879–1900.
- Cantu D., Blanco-Ulate B., Yang L., Labavitch J.M., Bennett A.B. & Powell A.L. (2009) Ripening-regulated susceptibility of tomato fruit to *Botrytis cinerea* requires NOR but not RIN or ethylene. *Plant Physiology* **150**, 1434–1449.
- Choquer M., Fournier E., Kunz C., Levis C., Pradier J.M., Simon A. & Viaud M. (2007) *Botrytis cinerea* virulence factors: new insights into a necrotrophic and polyphagous pathogen. *FEMS Microbiology Letters* **277**, 1–10.
- Coertze S. & Holz G. (2002) Epidemiology of *Botrytis cinerea* on grape: wound infection by dry, airborne conidia. *South African Journal for Enology and Viticulture* **23**, 72–77.
- Conesa A., Götz S., García-Gómez J.M., Terol J., Talón M. & Robles M. (2005) Blast2GO: a universal tool for annotation, visualization and analysis in functional genomics research. *Bioinformatics* **21**, 3674–3676.
- Costa A., Drago I., Behera S., Zottini M., Pizzo P., Schroeder J.I., Pozzan T. & Lo S.F. (2010) H<sub>2</sub>O<sub>2</sub> in plant peroxisomes: an *in vivo* analysis uncovers a Ca<sup>2+</sup>-dependent scavenging system. *The Plant Journal* **62**, 760–772.
- Dadakova K., Havelkova M., Kurkova B., Tolokova I., Kasparovsky T., Zdrahal Z. & Lochman J. (2015) Proteome and transcript analysis of *Vitis vinifera* cell cultures subjected to *Botrytis cinerea* infection. *Journal of Proteomics* **119**, 143–153.
- Dalmis B., Schumacher J., Moraga J., Le Pecheur P., Tudzynski B., Collado I.G. & Viaud M. (2011) The *Botrytis cinerea* phytotoxin botcinic acid requires two polyketide synthases for production and has a redundant role in virulence with botrydial. *Molecular Plant Pathology* **12**, 564–579.
- De Cremer K., Mathys J., Vos C., Froenicke L., Michelmore R.W., Cammue B.P. & De Coninck B. (2013) RNAseq-based transcriptome analysis of *Lactuca sativa* infected by the fungal necrotroph *Botrytis cinerea*. *Plant, Cell & Environment* **36**, 1992–2007.
- Deytieux-Belleau C., Geny L., Roudet J., Mayet V., Donèche B. & Fermaud M. (2009) Grape berry skin features related to ontogenic resistance to *Botrytis cinerea*. *European Journal of Plant Pathology* **125**, 551–563.
- Du Z., Zhou X., Ling Y., Zhang Z. & Su Z. (2010) agriGO: a GO analysis toolkit for the agricultural community. *Nucleic Acids Research* **38**, W64–W70.
- Eichorn K.W. & Lorenz D.H. (1977) Phänologische entwicklungsstadien der rebe. *Nachrichtenblatt des Deutschen Pflanzenschutzdienstes* **29**, 119–120.
- Elmer P.A.G. & Michailides T.M. (2004) Epidemiology of *Botrytis cinerea* in orchard and vine crops. In *Botrytis: Biology, Pathology and Control* (eds Elad Y., Williamson B., Tudzynski P. & Delan N.), pp. 234–272. Kluwer Academic, Dordrecht, the Netherlands.
- Espino J.J., Gutiérrez-Sánchez G., Brito N., Shah P., Orlando R. & González C. (2010) The *Botrytis cinerea* early secretome. *Proteomics* **10**, 3020–3034.
- Favaron F., Lucchetta M., Odorizzi S., da Cunha A.T.P. & Sella L. (2009) The role of grape polyphenols on *trans*-resveratrol activity against *Botrytis cinerea* and of fungal laccase on the solubility of putative grape PR proteins. *Journal of Plant Pathology* **91**, 579–588.
- Giannakis C., Bucheli C.S., Skene K.G.M., Robinson S.P. & Scott N.S. (1998) Chitinase and beta-1,3-glucanase in grapevine leaves: a possible defence against powdery mildew infection. *Australian Journal of Grape and Wine Research* **4**, 14–22.
- Gilbert H.J. (2010) The biochemistry and structural biology of plant cell wall deconstruction. *Plant Physiology* **153**, 444–455.
- Godfrey D., Able A.J. & Dry I.B. (2007) Induction of a grapevine germin-like protein (*VvGLP3*) gene is closely linked to the site of *Erysiphe necator* infection: a possible role in defense? *Molecular Plant-Microbe Interactions* **20**, 1112–1125.
- Goetz G., Fkyerat A., Metais N., Kunz M., Tabacchi R., Pezet R. & Pont V. (1999) Resistance factors to grey mould in grape berries: identification of some phenolics inhibitors of *Botrytis cinerea* stilbene oxidase. *Phytochemistry* **52**, 759–767.
- Grimple J., Van Hemert J., Carbonell-Bejerano P., Diaz-Riquelme J., Dickerson J., Fennell A., ... Martínez-Zapater J.M. (2012) Comparative analysis of grapevine whole-genome gene predictions, functional annotation, categorization and integration of the predicted gene sequences. *BMC Research Notes* **5**, 213.
- Guetsky R., Kobiler I., Wang X., Perlman N., Gollop N., Avila-Quezada G., ... Prusky D. (2005) Metabolism of the flavonoid epicatechin by laccase of *Colletotrichum gloeosporioides* and its effect on pathogenicity on avocado fruits. *Phytopathology* **95**, 1341–1348.
- Hammerbacher A., Ralph S.G., Bohlmann J., Fenning T.M., Gershenzon J. & Schmidt A. (2011) Biosynthesis of the major tetrahydroxystilbenes in spruce, astringin and isorhapontin, proceeds via resveratrol and is enhanced by fungal infection. *Plant Physiology* **157**, 876–890.
- Hellemans J., Mortier G., De Paep A., Speleman F. & Vandesompele J. (2007) qBase relative quantification framework and software for management and automated analysis of real-time quantitative PCR data. *Genome Biology* **8**, R19.
- Höll J., Vannozzi A., Czemplak S., D'Onofrio C., Walker A.R., Rausch T., ... Bogs J. (2013) The R2R3-MYB transcription factors MYB14 and MYB15 regulate stilbene biosynthesis in *Vitis vinifera*. *Plant Cell* **25**, 4135–4149.
- Jaillon O., Aury J.M., Noel B., Policriti A., Clepet C., Casagrande A., ... French-Italian Public Consortium for Grapevine Genome Characterization,

- French-Italian Public Consortium for Grapevine Genome Characterization (2007) The grapevine genome sequence suggests ancestral hexaploidization in major angiosperm phyla. *Nature* **449**, 463–467.
- Jarvis W.R. (1962) The infection of strawberry and raspberry fruits by *Botrytis cinerea* Fr. *Annals of Applied Biology* **50**, 569–575.
- Jarvis W.R. (1994) Latent infections in the pre- and post-harvest environment. *Hortscience* **29**, 749–751.
- Jeandet P., Bessis R., Sbaghi M. & Meunier P. (1995) Production of the phytoalexin resveratrol by grapes as a response to *Botrytis* attack under natural conditions. *Journal of Phytopathology* **143**, 135–139.
- Jersch S., Scherer C., Huth G. & Schlösser E. (1989) Proanthocyanidins as basis for quiescence of *Botrytis cinerea* in immature strawberry fruits. *Z. Pflanzenkrankh Pflanzenschutz* **96**, 365–378.
- van Kan J.A.L. (2006) Licensed to kill: the lifestyle of a necrotrophic plant pathogen. *Trends Plant Science* **11**, 247–253.
- van Kan J.A.L., Shaw M.W. & Grant-Downton R.T. (2014) *Botrytis* species: relentless necrotrophic thugs or endophytes gone rogue? *Molecular Plant Pathology* **15**, 957–961.
- van Kan J.A.L., Stassen J.H.M., Mosbach A., van Der Lee T.A.J., Faino L., Farmer A.D., ... Scalliet G. (2016) A gapless genome sequence of the fungus *Botrytis cinerea*. *Molecular Plant Pathology*. DOI:10.1111/mpp.12384.
- Keller M., Viret O. & Cole M. (2003) *Botrytis cinerea* infection in grape flowers: defense reaction, latency and disease expression. *Phytopathology* **93**, 316–322.
- Kelloniemi J., Trouvelot S., Heloir M.C., Simon A., Dalmais B., Frettinger P., ... Viaud M. (2015) Analysis of the molecular dialogue between gray mold (*Botrytis cinerea*) and grapevine (*Vitis vinifera*) reveals a clear shift in defense mechanisms during berry ripening. *Molecular Plant-Microbe Interactions* **28**, 1167–1180.
- Kemmerling B., Schwedt A., Rodríguez P., Mazzotta S., Frank M., Abu Q.S., ... Nürnberger T. (2007) The BRI1-associated kinase 1, BAK1, has a Brassinoli-independent role in plant cell-death control. *Current Biology* **17**, 1116–1122.
- Kretschmer M., Kassemeyer H.H. & Hahn M. (2007) Age-dependent grey mould susceptibility and tissue-specific defence gene activation of grapevine berry skins after infection by *Botrytis cinerea*. *Journal of Phytopathology* **155**, 258–263.
- Langcake P. (1981) Disease resistance of *Vitis* spp. and the production of the stress metabolites resveratrol, epsilon-viniferin, alpha-viniferin and pterostilbene. *Physiological Plant Pathology* **18**, 213–226.
- Law C.W., Chen Y., Shi W. & Smyth G.K. (2014) Voom: precision weights unlock linear model analysis tools for RNA-Seq read counts. *Genome Biology* **15**, R29.
- Lebel S., Schellenbaum P., Walter B. & Maillot P. (2010) Characterisation of the *Vitis vinifera* PR10 multigene family. *BMC Plant Biology* **10**, 184.
- Lee P.P., Messersmith P.B., Israelachvili J.N. & Waite J.H. (2011) Mussel inspired adhesives and coatings. *Annual Review of Materials Research* **41**, 99–132.
- Leroch M., Kleber A., Silva E., Coenen T., Koppenhöfer D., Shmaryahu A., Valenzuela P.D.T. & Hahn M. (2013) Transcriptome profiling of *Botrytis cinerea* conidial germination reveals upregulation of infection-related genes during the prepenetration stage. *Eukaryotic Cell* **12**, 614–626.
- Leroch M., Mernke D., Koppenhöfer D., Schneider P., Mosbach A., Doehlemann G. & Hahn M. (2011) Living colors in the gray mold pathogen *Botrytis cinerea*: codon-optimized genes encoding green fluorescent protein and mCherry, which exhibit bright fluorescence. *Applied and Environmental Microbiology* **77**, 2887–2897.
- Liao Y., Smyth G.K. & Shi W. (2013) The Subread aligner: fast, accurate and scalable read mapping by seed-and-vote. *Nucleic Acids Research* **41**, e108.
- Liao Y., Smyth G.K. & Shi W. (2014) featureCounts: an efficient general-purpose program for assigning sequence reads to genomic features. *Bioinformatics* **30**, 923–930.
- Lijavetzky D., Carbonell-Bejerano P., Grimplet J., Bravo G., Flores P., Fenoll J., ... Martínez-Zapater J.M. (2012) Berry flesh and skin ripening features in *Vitis vinifera* as assessed by transcriptional profiling. *PLoS One* **7**, e39547.
- Liu Z.Y., Zhuang C.X. & Sheng S.J. (2011) Overexpression of a resveratrol synthase gene (PcRS) from *Polygonum cuspidatum* in transgenic *Arabidopsis* causes the accumulation of trans-piceid with antifungal activity. *Plant Cell Reports* **30**, 2027–2036.
- Malacarne G., Vrhovsek U., Zulini L., Cestaro A., Stefanini M., Mattivi F., ... Moser C. (2011) Resistance to *Plasmopara viticola* in a grapevine segregating population is associated with stilbenoid accumulation and with specific host transcriptional responses. *BMC Plant Biology* **11**, 114.
- Marrs K.A. (1996) The functions and regulation of glutathione S-transferases in plants. *Annual Review of Plant Physiology and Plant Molecular Biology* **47**, 127–158.
- Martin M. (2011) Cutadapt removes adapter sequences from high-throughput sequencing reads. *EMBnetjournal* **17**, 10–12.
- McClellan W.D. & Hewitt W.B. (1973) Early *Botrytis* rot of grapes: time of infection and latency of *Botrytis cinerea* Pers. in L. *Phytopathology* **63**, 1151–1157.
- McNicol R.J. & Williamson B. (1989) Systemic infection of blackcurrant flowers by *Botrytis cinerea* and its possible involvement in premature abscission of fruits. *Annals of Applied Biology* **114**, 243–254.
- Merz P.R., Moser T., Höll J., Kortekamp A., Buchholza G., Zyprian E. & Bogs J. (2015) The transcription factor VvWRKY33 is involved in the regulation of grapevine (*Vitis vinifera*) defense against the oomycete pathogen *Plasmopara viticola*. *Physiologia Plantarum* **153**, 365–380.
- Mlikota-Gabler F., Smilanick J.L., Mansour M., Ramming D.W. & Mackey B.E. (2003) Correlation of morphological, anatomical, and chemical features of grape berries with resistance to *Botrytis cinerea*. *Phytopathology* **93**, 1263–1273.
- Mohnen D. (2008) Pectin structure and biosynthesis. *Current Opinion in Plant Biology* **11**, 226–277.
- Monteiro S., Barakat M., Picarra-Pereira M.A., Teixeira A.R. & Ferreira R.B. (2003) Osmotin and thaumatin from grape: a putative general defense mechanism against pathogenic fungi. *Phytopathology* **93**, 1505–1512.
- Moretto M., Sonogo P., Dierckxssens N., Brilli M., Bianco L., Ledezma-Tejeida D., ... Engelen K. (2016) COLOMBOS v3.0: leveraging gene expression compendia for cross-species analyses. *Nucleic Acids Research* **44**, D620–D623.
- Mullins M.G. & Rajaskekaren K. (1981) Fruiting cuttings: revised method for producing test plants of grapevine cultivars. *American Journal of Enology and Viticulture* **32**, 35–40.
- Nagpala E.G., Guidarelli M., Gasperotti M., Masuero D., Bertolini P., Vrhovsek U. & Baraldi E. (2016) Polyphenols variation in fruits of the susceptible strawberry cultivar Alba during ripening and upon fungal pathogen interaction and possible involvement in unripe fruit tolerance. *Journal of Agricultural and Food Chemistry* **64**, 1869–1878.
- Nair N.G., Guilbaud-Oulton S., Barchia I. & Emmett R. (1995) Significance of carry over inoculum, flower infection and latency on the incidence of *Botrytis cinerea* in berries of grapevines at harvest *Vitis vinifera* in New South Wales. *Australian Journal of Experimental Agriculture* **35**, 1177–1180.
- Naoumkina M.A., Zhao Q., Gallego-Giraldo L., Dai X., Zhao P.X. & Dixon R.A. (2010) Genome-wide analysis of phenylpropanoid defence pathways. *Molecular Plant Pathology* **11**, 829–846.
- Noda J., Brito N. & Gonzalez C. (2010) The *Botrytis cinerea* xylanase Xyn11A contributes to virulence with its necrotizing activity, not with its catalytic activity. *BMC Plant Biology* **10**, 38.
- Padgett M. & Morrison J.C. (1990) Changes in the grape berry exudates during fruit development and their effect on the mycelial growth of *Botrytis cinerea*. *Journal of the American Society for Horticultural Science* **115**, 269–273.
- Pezet R., Perret C., Jean-Denis J.B., Tabacchi R., Gindro K. & Viret O. (2003a)  $\delta$ -Viniferin, a resveratrol dehydrodimer: one of the major stilbenes synthesized by stressed grapevine leaves. *Journal of Agricultural and Food Chemistry* **51**, 5488–5492.
- Pezet R., Viret O., Perret C. & Tabacchi R. (2003b) Latency of *Botrytis cinerea* Pers.: Fr. and biochemical studies during growth and ripening of two grape berry cultivars, respectively susceptible and resistant to grey mould. *Journal of Phytopathology* **151**, 208–214.
- Prusky D. (1996) Pathogen quiescence in postharvest diseases. *Annual Review of Phytopathology* **34**, 413–434.
- Prusky D., Alkan N., Mengiste T. & Fluhr R. (2013) Quiescent and necrotrophic lifestyle choice during postharvest disease development. *Annual Review of Phytopathology* **51**, 155–176.
- Prusky D. & Lichter A. (2007) Activation of quiescent infections by postharvest pathogens during transition from the biotrophic to the necrotrophic stage. *FEMS Microbiology Letters* **268**, 1–8.
- Puhl I. & Treutter D. (2008) Ontogenetic variation of catechin biosynthesis as basis for infection and quiescence of *Botrytis cinerea* in developing strawberry fruits. *Journal of Plant Diseases and Protection* **115**, 247–251.
- Rieu I. & Powers S.J. (2009) Real-time quantitative RT-PCR: design, calculations, and statistics. *Plant Cell* **2**, 1031–1033.
- Rolke Y., Liu S., Quiddle T., Williamson B., Schouten S., Weltring K.M., ... Tudzynski P. (2004) Functional analysis of H<sub>2</sub>O<sub>2</sub>-generating systems in *Botrytis cinerea*: the major Cu–Zn–superoxide dismutase (BCSOD1) contributes to virulence on French bean, whereas a glucose oxidase (BCGOD1) is dispensable. *Molecular Plant Pathology* **5**, 17–27.
- Rossi F.R., Garriz A., Marina M., Romero F.M., Gonzalez M.E., Collad I.G. & Pieckenstein F.L. (2011) The sesquiterpene botrydial produced by *Botrytis cinerea* induces the hypersensitive response on plant tissues and its action is

- modulated by salicylic acid and jasmonic acid signaling. *Molecular Plant–Microbe Interactions* **24**, 888–896.
- Ruijter J.M., Ramakers C., Hoogaars W.M., Karlen Y., Bakker O., van den Hoff M.J. & Moorman A.F. (2009) Amplification efficiency: linking baseline and bias in the analysis of quantitative PCR data. *Nucleic Acids Research* **37**, e45.
- Schouten A., Tenberge K.B., Vermeer J., Stewart J., Wagemakers C.A.M., Williamson B. & van Kan J.A.L. (2002a) Functional analysis of an extracellular catalase of *Botrytis cinerea*. *Molecular Plant Pathology* **3**, 227–238.
- Schouten A., Wagemakers L., Stefanato F.L., van der Kaaij R.M. & van Kan J.A.L. (2002b) Resveratrol acts as a natural fungicide and induces self-intoxication by a specific laccase. *Molecular Microbiology* **43**, 883–894.
- Schumacher J. (2012) Tools for *Botrytis cinerea*: new expression vectors make the gray mold fungus more accessible to cell biology approaches. *Fungal Genetics and Biology* **49**, 483–497.
- Schumacher J., Simon A., Cohrs K.C., Viaud M. & Tudzynski P. (2014) The transcription factor BcLTF1 regulates virulence and light responses in the necrotrophic plant pathogen *Botrytis cinerea*. *PLoS Genetics* **10**, e1004040.
- Shaw M.W., Emmanuel C.J., Emilda D., Terhem R.B., Shafia A., Tsamadi D., ... van Kan J.A.L. (2016) Analysis of cryptic, systemic *Botrytis* infections in symptomless hosts. *Frontiers in Plant Science* **7**, 625.
- Smith J.E., Mengesha B., Tang H., Mengiste T. & Bluhm B.H. (2014) Resistance to *Botrytis cinerea* in *Solanum lycopersicoides* involves widespread transcriptional reprogramming. *BMC Genomics* **15**, 334.
- Smyth G.K. (2004) Linear models and empirical Bayes methods for assessing differential expression in microarray experiments. *Statistical Applications in Genetics and Molecular Biology* **3**, 3.
- Thimm O., Bläsing O., Gibon Y., Nagel A., Meyer S., Krüger P., ... Stitt M. (2004) MAPMAN: a user-driven tool to display genomics data sets onto diagrams of metabolic pathways and other biological processes. *The Plant Journal* **37**, 914–939.
- Vandesompele J., De Preter K., Pattyn F., Poppe B., van Roy N., De Paepe A. & Speleman F. (2002) Accurate normalization of real-time quantitative RT-PCR data by geometric averaging of multiple internal control genes. *Genome Biology* **3**, RESEARCH0034.
- Vannozzi A., Dry I.B., Fasoli M., Zenoni S. & Lucchin M. (2012) Genome-wide analysis of the grapevine stilbene synthase multigenic family: genomic organization and expression profiles upon biotic and abiotic stresses. *BMC Plant Biology* **12**, 130.
- Velasco R., Zharkikh A., Troglio M., Cartwright D.A., Cestaro A., Pruss D., ... Viola R. (2007) A high quality draft consensus sequence of the genome of a heterozygous grapevine variety. *PLoS One* **2**, e1326.
- Volodarsky D., Leviatan N., Otcheretianski A. & Fluhr R. (2009) HORMONOMETER: a tool for discerning transcript signatures of hormone action in the *Arabidopsis* transcriptome. *Plant Physiology* **150**, 1796–1805.
- Vrhovsek U., Masuero D., Gasperotti M., Franceschi P., Caputi L., Viola R. & Mattivi F. (2012) A versatile targeted metabolomics method for the rapid quantification of multiple classes of phenolics in fruits and beverages. *Journal of Agricultural and Food Chemistry* **60**, 8831–8840.
- Waite J.H., Hansen D.C. & Little K.T. (1989) The glue protein of ribbed mussels (*Geukensia demissa*): a natural adhesive with some features of collagen. *Journal of Comparative Physiology B* **159**, 517–525.
- Weng K., Li Z.Q., Liu R.Q., Wang L., Wang Y.J. & Xu Y. (2014) Transcriptome of *Erysiphe necator* infected *Vitis pseudoreticulata* leaves provides insight into grapevine resistance to powdery mildew. *Horticulture Research* **1**, 14049.
- Wiermer M., Feys B.J. & Parker J.E. (2005) Plant immunity: the EDS1 regulatory node. *Current Opinion in Plant Biology* **8**, 383–389.
- Williamson B., McNicol R.J. & Dolan A. (1987) The effect of inoculating flowers and developing fruits with *Botrytis cinerea* on post-harvest grey mould of red raspberry. *Annals of Applied Biology* **111**, 285–294.
- Williamson B., Tudzynski B., Tudzynski P. & van Kan J.A.L. (2007) *Botrytis cinerea*: the cause of grey mould disease. *Molecular Plant Pathology* **8**, 561–580.
- Zhang W., Fraiture M., Kolb D., Löffelhardt B., Desaki Y., Boutrot F.F., ... Brunner F. (2013) *Arabidopsis* RECEPTOR-LIKE PROTEIN30 and receptor-like kinase SUPPRESSOR OF BIR1-1/EVERSHED mediate innate immunity to necrotrophic fungi. *Plant Cell* **25**, 4227–4241.
- Zhang L., Thiewes H. & van Kan J.A.L. (2011) The D-galacturonic acid catabolic pathway in *Botrytis cinerea*. *Fungal Genetics and Biology* **48**, 990–997.
- Zhao Q., Nakashima J., Chen F., Yin Y., Fu C., Yun J., ... Dixon R.A. (2013) Laccase is necessary and nonredundant with peroxidase for lignin polymerization during vascular development in *Arabidopsis*. *Plant Cell* **25**, 3976–3987.

Received 16 November 2016; accepted for publication 13 February 2017

## SUPPORTING INFORMATION

Additional Supporting Information may be found online in the supporting information tab for this article.

Supporting Information Figure S1. Droplets of conidial suspension on the grapevine flowers.

Supporting Information Figure S2. PDB-cultured *B. cinerea* conidia.

Supporting Information Figure S3. Standard curves of *B. cinerea* and *V. vinifera* genomic DNA.

Supporting Information Figure S4. Z-stack images of *Botrytis* infecting a grapevine flower.

Supporting Information Figure S5. Effects of washing and surface sterilization on the viability of *B. cinerea*.

Supporting Information Figure S6. Egression of *B. cinerea* at ripening.

Supporting Information Figure S7. Immature berries bagged for 2 weeks to test *B. cinerea* egression.

Supporting Information Figure S8. Volcano plots of grapevine genes.

Supporting Information Figure S9. Hormonal signatures based on transcriptomic data.

Supporting Information Data S1. List of qPCR primers.

Supporting Information Data S2. Summary of reads of RNA-Seq.

Supporting Information Data S3. Expression profile of *V. vinifera* flower upon *B. cinerea* infection.

Supporting Information Data S4. Differentially expressed genes of *V. vinifera*.

Supporting Information Data S5. List of genes used to validate the expression values of RNA-Seq.

Supporting Information Data S6. Gene ontology terms enriched in the differentially expressed grapevine genes.

Supporting Information Data S7. MapMan BINs enriched in the differentially expressed grapevine genes.

Supporting Information Data S8. List of differentially expressed *V. vinifera* genes belonging to the biotic stress functional categories.

Supporting Information Data S9. Concentration of polyphenolic secondary metabolites.

Supporting Information Data S10. Number of raw reads of *B. cinerea* transcripts expressed in the infected grapevine flower.

Supporting Information Data S11. Selection of the *B. cinerea* genes defined as expressed *in planta*.

Supporting Information Data S12. Gene ontology annotation of *B. cinerea* genes expressed *in planta*.